The cobalt-nickel pertraction refinery to process recycled spent catalysts leach solutions

N Mans

orcid.org 0000-0001-9379-9111

Dissertation submitted in partial fulfilment of the requirements for the degree *Masters of Science in Chemistry* at the North-West University

Supervisor: Mr DJ van der Westhuizen

Co-supervisor: Prof HM Krieg

Graduation May 2019

24244430

Conference contribution from this study

Article

Mans, N.; van der Westhuizen, D. J.; Bruinsma, D.; Cole, P.; du Toit, J.; Munnik, E.; Coates, A.; Coetzee, V.; Krieg, H. M. In *Cobalt-Nickel Pertraction Refinery to Process Pregnant Leach Solution from Recycled Spent Catalysts Part 1: Cobalt extraction from a Binary System*, Copper Cobalt Africa, incorporating the 9th Southern African Base Metals Conference, Livingstone, Zambia, 10-12 July; Southern African Institute of Mining and Metallurgy: Livingstone, Zambia, 2018; pp 363-374.

Presentation

Mans, N. van der Westhuizen, D.J. Bruinsma, D. Cole, P. du Toit, J. Munnik, E. Coates, A. Coetzee, V and Krieg, H.M. (2018). Cobalt-Nickel Pertraction Refinery to Process Pregnant Leach Solution from Recycled Spent Catalysts Part 1: Cobalt extraction from a Binary System. Copper Cobalt Africa, incorporating the 9th Southern African Base Metals Conference, Livingstone, Zambia, Southern African Institute of Mining and Metallurgy.

Preface

"Like success, failure is many things to many people. With positive mental attitude, failure is a learning experience, a rung on the ladder, a plateau at which to get your thoughts in order and prepare to try again."

-W. Clement Stone-

"The greatest glory in living lies not in never failing, but in rising every time we fall."

-N. Mandela-

"You don't learn to walk by following rules. You learn by doing and falling over."

-R. Branson-

Throughout the course of this project I have learnt that one of the most important personal traits is the ability to not be discouraged by failure. Failure should, instead, serve as motivation to try again. Without life's failures, its victories would be obsolete.

I would like to thank the following people:

My supervisor, Mr. Derik J van der Westhuizen. Thank you for your guidance, friendship and devotion during this project. You have taught me that most of the complications encountered during research, very much like most of the problems encountered in life, can be dealt with through logical thought and a bit of humour. The opportunities that you create for your students do not only help us to grow as researchers, but also as individuals.

My co-supervisor, Prof Henning M Krieg. I would like to thank you for leading by example and for your continuous support during this project. I admire your ability to maintain a professional working environment whilst simultaneously keeping the individualism of each of your students in mind.

To my colleagues, who became close friends, both within and outside of the Membrane Technology group. The coffee breaks and lunches have become valuable brainstorming and venting sessions. Your support has become essential for my emotional well-being.

My parents, Alta and Rudie Mans. Thank you for celebrating each of my victories as your own. Your support and sacrifices, both during this project and the years that led up to it, are greatly appreciated.

My friend and colleague Wouter-Dirk van der Spoel Badenhorst. Thank you for your support, albeit at the cost of a snarky comment, during this project. Your involvement has been essential to the success achieved.

And the following institutions:

The CRB and the North-West University Potchefstroom campus for the use of their facilities.

Minemet PTY(LTD) for supplying the industrial sample used in this study.

ChemQuest for supplying the Shellsol 2325 diluent.

ABSTRACT

Over the last two years, the cobalt (Co) price has increased considerably. The observed increase can be attributed to the increase in demand of lithium-ion batteries (LIBs) of which Co forms an integral part. As a consequence of the envisaged steady rise in the demand for LIBs, a steady increase in the demand for Co is expected. Currently, more than 50 % of the world's produced Co is obtained from the Democratic Republic of the Congo. This supply chain is, however, threatened by political instability, geopolitics, corruption, child labour and artisanal mining. An alternative source could be, for example, Co-rich spent hydro-treatment catalysts, which would however, require new cobalt-nickel refining capacities. This creates the perfect opportunity for the industrial introduction of a novel solvent extraction (SX) based technology, i.e. pertraction (PX), also known as membrane-based solvent extraction.

During this study, liquid-liquid extraction (LLE) data were obtained and used to identify optimum conditions for the extraction, scrubbing and stripping of Co from a pregnant leach solution (PLS) obtained from spent hydro-treatment catalysts. Accordingly, a solvent containing 22 wt% of the extractant Cyanex272 (C272), of which 50 % was pre-neutralized with NH_4OH, was able to extract 96 % of the Co (with a 5 % co-extraction of Ni) from the PLS provided by Minemet PTY(LTD) resulting in a raffinate containing a Ni purity of 97 %. When scrubbing the loaded organic phase in an organic to aqueous ratio (O/A) of 30:1 with a 50 g/L Co solution at a pH of 5.0, the Co purity was increased by 12 %. Simultaneously, virtually all the co-extracted Ni was scrubbed from the organic phase. Finally, using a 0.1 M H_2SO_4 striping liquor, 98 % of Co was stripped from the scrubbed organic, resulting in a scrub liquor containing 5.7 g/L Co at a purity of 97 %. Alternatively, when using a 0.2 M H_2SO_4 stripping liquor, 100 % of the Co was recovered from the scrubbed organic, resulting in a scrub liquor containing 5.8 g/L Co at a purity of 96 %.

The optimised conditions from the LLE data were subsequently used when optimising the mass transfer during Co PX processing. According to the resistance in series model, three PX design parameters are of importance: mass transfer coefficient at aqueous interphase (k_{Aq}), mass transfer coefficient of the solvent in the pores and lumen combined (k_{MO}) and the distribution (D). It was firstly shown that an increase in the distribution coefficient lead to enhanced mass transfer kinetics of Co, where a 50 % increase in k_{ov} was observed when increasing the C272 from 9 to 22 wt%. It was then found that an increase in extractant concentration also led to increased mass transfer kinetics. Lastly, it was shown that the largest mass transfer resistance was due to the transport and diffusion in the module and not due to reaction kinetics.

Applying the data (feed composition analysis, loading isotherms, mass transfer kinetics and mass balance) to the process models, a conceptual design of the extraction section of a PX refinery was proposed. Using the optimised conditions, a membrane area of 2125 m^2 would be required to obtain a Ni purity of 99.9 % in the raffinate. Since the Liqui-Cel™ 14x40 XF modules delivers a contact area of 373 m^2 each, 5.7 of these modules in series would attain the required stream of 200 L/h. Using an integer of six modules, a raffinate purity of 99.99 % would be attainable.

KEYWORDS: Cobalt, Nickel, Solvent extraction, Membrane-based solvent extraction, Pertraction, Cyanex 272, Conceptual pertraction plant design.

List of Figures

List of Tables

Nomenclature and symbols

$\hat{z}_i$	mole fraction in solvent (mol/mol)
Δp_{bubble}	Membrane bubble point pressure (kPa)
Δp_{total}	Total pressure drop over module (kPa)
A	Area of membrane contactor (m^2)
C272	Cyanex 272 (bis(2,4,4-trimethylpentyl)phosphinic acid)
Co metal	Metallic cobalt
D	Distribution coefficient
D_F	Feed side distribution coefficient
D_{gm}	Geometric mean of distribution coefficients
D_R	Raffinate side distribution coefficient
DRC	Democratic Republic of the Congo
E^0	Standard reduction potential (V)
Fe	Iron
Feed	Aqueous feed stream
ICP-OES	Inductively coupled plasma optical emission spectroscopy
IX	Ion exchange
k_{Aq}	Mass transfer coefficient at aqueous interphase (m/s)
k_M	Membrane mass transfer coefficient (m/s)
k_{Org}	Mass transfer coefficient at solvent interphase (m/s)
k_{ov}	Overall mass transfer coefficient (m/s)
L	Dimensionless position in pertraction column
LIBs	Lithium ion batteries
LLE	Liquid-liquid extraction
LME	London metal exchange
Lumen	Area inside membrane hollow fibres
Mixbox	Aqueous/Organic emulsion in mixer
Module	Membrane contactor
O/A ratio:	Organic to aqueous ratio
PLS	Pregnant leach solution
pptn.	Precipitation
PX	Pertraction or also known as Membrane-based solvent extraction
Q_{Aq}	Aqueous flow rate (L/h; m^3/s)
Q_{Org}	Solvent flow rate (L/h; m^3/s)
Q_{Org}/Q_{Aq}	Organic to aqueous flow rate
Raffinate	Aqueous feed stream after contact with solvent
SF	Separation factor

Shell	Area surrounding membrane fibres
SLM	Solvent or supported liquid membrane
Solvent	Organic feed stream
StL	Strip liquor
SX	Solvent extraction
t	Time (s)
V_{Aq}	Feed volume (L)
V_{Lumen}	Lumen volume (mL)
V_{Org}	Solvent volume (L)
V_{Shell}	Shell volume (mL)
x	Concentration in the feed (g/L)
x_i	Aqueous interphase concentration (g/L)
y	Concentration in the extract (g/L)
y_i	Organic interphase concentration (g/L)
μ_0	Viscosity at 20 ºC (mPa.s)

Table of contents

CHAPTER 1

INTRODUCTION

1.1) Background

Lithium ion batteries (LIBs), which serve as the preferred power source for portable electronic devices, electric vehicles and as an alternative energy storage solution, contain lithium (Li) compounds as the cathodic material. The cathode composition varies between the various LIBs that are available, but generally contain 5 – 7 % Li, 5 – 20 % cobalt (Co) and 5 – 10 % nickel (Ni).[1] Due to the proliferation of both portable electronic devices and electrical vehicles, the Co price has increased considerably over the last two years.[2] As a result, both mining- and metallurgical processing industries started looking for new Co sources. In line with recent developments for other metals, a possible source could be by recycling Co-rich spent hydro-treatment catalysts. The recycling of Co from such spent hydro-treatment catalysts will, however, require new cobalt-nickel (Co-Ni) refining capacities; which are currently dominated by China.[3] This is the perfect opportunity for the industrial introduction of a novel solvent extraction (SX) based technology, i.e. pertraction (PX), also known as membrane-based solvent extraction.[4]

It is known that SX is one of the major separation and purification unit operations in hydrometallurgy,[5] partially based on the range of selective extractants that are commercially available. Additionally, the technique offers low capital- and operating costs.[6] For SX, mixer-settlers and extraction columns are the conventional process configurations. More recently, PX technology using a membrane contactor has been introduced at laboratory scale, where the membrane acts as a semipermeable barrier between the aqueous and organic phases.[7] While in both SX and PX metals are selectively transferred from the aqueous to the organic phase during extraction, in PX the transfer occurs via a membrane contactor that avoids the requirement of having to mix both phases. During scrubbing and stripping, transfer of the metal species is again done selectively, this time in the reverse direction with or without a membrane.

PX should not be confused with a solvent supported liquid membrane (SLM) process, where only the porous membrane is filled with solvent and both sides (shell and lumen) are aqueous.[8] It is known that the SLM configuration is highly unstable due to the irreversible loss of solvent.[9] In contrast, using the PX configuration, where the one side of the membrane is filled with the aqueous phase and the other side with the organic phase, solvent losses are easily prevented by applying a small

overpressure on the non-wetting side of the membrane.[10] In the case of accidental breakthrough, the entrained phase will automatically return to the side of the membrane where it is located due to the overpressure. The mixing requirement of SX showcases numerous disadvantages such as foaming, flooding, unloading, the need for density differences, and stable emulsion formation which requires additional management during industrial operations.[7] PX, on the other hand, which is a non-dispersive technique, can be used to overcome these specific challenges associated with SX. Additional industrial advantages that PX offers over conventional SX processing includes i) reduction in plant size and cost as no settlers are required, ii) reduction in metal lock-up on plant, iii) reduction in maintenance costs because of the reduction in rotating equipment, and iv) increased safety because PX is a closed system while solvent holdup is reduced.

Minemet PTY(LTD) is a South African-based home-grown niche chemical company that recycles spent hydro-treatment catalysts from local oil refineries into useful products, including products supplied to local agricultural markets for seed enhancement and soil enrichment, pigments, and products for water treatment industries. The three main metals of value include Co, Ni and molybdenum (Mo), with iron (Fe) and manganese (Mn) as the major impurities present. During Minemet's traditional process, diagrammatically illustrated in Figure 1-1, organic residue, coke and sulfur are initially removed by calcination. Subsequently, the resulting mixture is fed to a smelter to obtain a Co-Ni-Mo-Fe-Mn alloy. A pregnant leach solution (PLS) is obtained from the aforementioned alloy via sulfuric acid leaching. The majority of Fe and Mn is then removed through precipitative oxidation, after which Mo is recovered using ion-exchange (IX). The resulting Co-Ni feed is fed into the SX circuit, where Co is selectively extracted using a Cyanex 272 (C272) solvent, leaving Ni in the raffinate. Currently, using the aforementioned process, Minemet PTY(LTD) produces Co and Ni products with purities of 95 and 98 %, respectively at a production rate of 80 L/h.

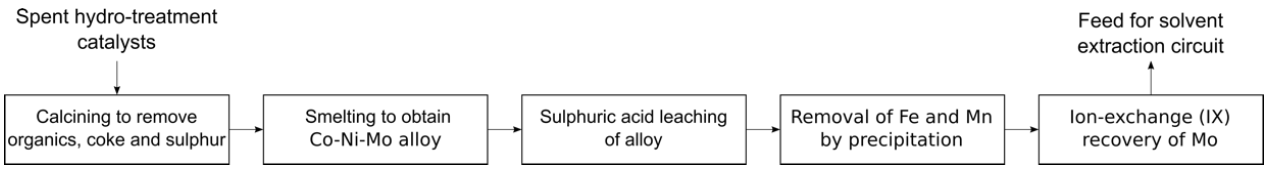

Figure 1-1. Minemet PTY(LTD) process to prepare the feed for the solvent extraction circuit.

In order to be suitable for the battery market, Minemet PTY(LTD) would have to produce a 99.9 % pure Ni solution and a battery-grade Co solution (99.8 %) at a target concentration of 50 g/L Co. Therefore, the design capacity of a PX plant should meet 200 L/h. A Co-Ni PX refinery would have the same block flow diagram as a conventional SX plant as shown in Figure 1-2. Accordingly, Co is initially extracted from the feed to obtain a raffinate with 99.9 % Ni purity. The co-extracted Ni is then scrubbed from the loaded solvent. Following Ni scrubbing, the scrubbed solvent is stripped using a sulfuric acid solution. The stripped solvent is then pre-neutralised using a base such as caustic soda or an ammonia solution and rerouted back to the extraction section.

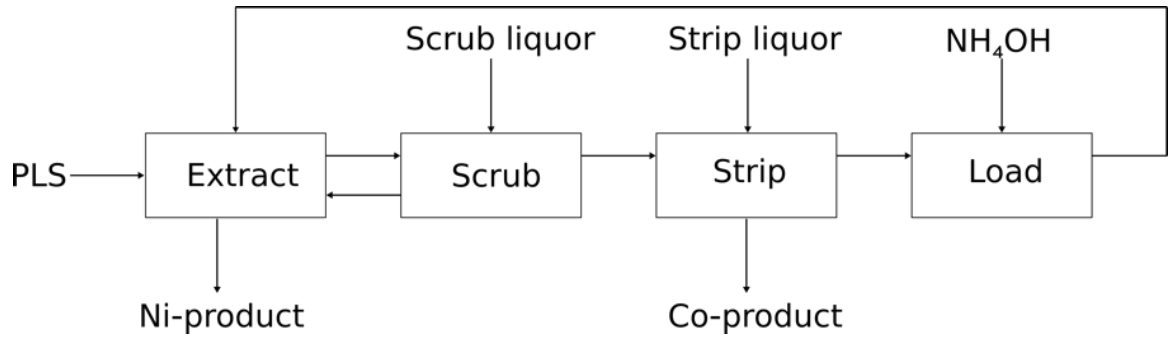

Figure 1-2. Flowsheet of a proposed pertraction cobalt-nickel refinery.

1.2) Problem statement

For Minemet to supply their products to the battery market, both the purity and production rate of these products would have to be increased. To achieve the required improvements, a PX refinery is proposed due to the numerous advantages that PX offers over traditional/conventional SX.

1.2.1) Research Questions

- Which solutions are suitable for extraction, scrubbing and stripping of Co from the industrial PLS?
- Can these suitable solutions be implemented for PX processing of the required metals?
- What chemical conditions are optimal/favourable for PX mass transfer kinetics?
- Which existing process models can be applied to PX results?
- Can these models be adapted for a continuous process and then be applied to conceptually design the extraction section of the PX plant?

1.2.2) Limitations

Due to the availability, remarkable selectivity (even at high Ni to Co concentration ratios) and stability of C272, it is unfeasible to apply another extractant industrially.[5, 11] This study was therefore limited to the application of C272 as extractant.

Currently electrowinning (EW) of Co is performed from dilute sulfuric acid solutions (pH values between 1.0 and 4.5) that contain Co in concentrations $\geq$ 50 g/L. The low pH values are required to improve process efficiency and the Co concentration for improved plating quality. As such the scrubbing and stripping liquors were limited to dilute sulfuric acid and a small portion of the advance electrolyte, respectively.

The mass transfer resistance during PX stripping is located at the module, as shown in Chapter 4. In order to optimise mass transfer kinetics during stripping, a hydrophilic membrane could be considered. Due to the unavailability of such a module, this was not considered for this study.

1.3) Aims and objectives

The aims of this project were to develop a process for the recovery and purification of Co from spent hydro-treatment catalysts using PX. The objectives were as follows:

- To identify optimal solvent, scrub liquor and strip liquor types and concentrations.
- To confirm use of optimal solutions in PX batch experiments.
- To optimise mass transfer kinetics using batch PX.
- To conceptually design an extraction circuit of a PX plant using LLE and PX results in conjunction with process models.

1.4) Overview of chapters

In Chapter 1, the increasing Co demand, which emphasises the importance of Co recovery from secondary sources, is discussed. The advantages that PX processing offers over SX are given, which serve as motivations for the proposed PX plant. The recovery of Co from spent hydro-treatment catalysts obtained from Minemet PTY(LTD) is discussed. After the introduction, the problem statement and limitations of the study are given. Finally, the aims and objectives are given.

In Chapter 2, an overview of the hydrometallurgical processing of Co is given. Initially, a general Co processing flowsheet is discussed, followed by a detailed discussion of the respective processing techniques that are used industrially for the purification and recovery of Co. An overview of PX is given, followed by the identification of a set of comprehensive models, which were to be used both for the interpretation of PX results and the conceptual design of the extraction circuit. Finally, the use of EW for Co metal production from the purified advance Co electrolyte is reviewed.

In Chapter 3, the general methods that were used for liquid-liquid extraction (LLE) and PX experiments, during the study, is discussed. Additionally, the specific conditions used for the respective LLE and PX experiments are given. Furthermore, the specifications of chemicals which were used to prepare synthetic aqueous solutions and solvents are given.

In Chapter 4, results of the LLE experiments, the PX batch runs and the proposed conceptual design are given. In the first section, LLE experiments were used to identify suitable solutions for extraction, scrubbing and stripping. After identification, the solutions were used to process the PLS supplied by Minemet PTY(LTD). The solutions were also used to perform PX batch experiments. The PX mass transfer kinetics were optimised and it was confirmed that the identified extraction-, scrubbing- and stripping solutions can be used for the PX processing of the industrial PLS. In the last section, the conceptual design of the extraction section of a PX refinery is proposed.

In Chapter 5, the results and conclusions drawn from Chapter 4 are discussed in line with the aforementioned aims and objectives. An evaluation of the project is given, and additional considerations and recommendations are discussed.

1.5) References

1. Shin, S. M.; Kim, N. H.; Sohn, J. S.; Yang, D. H.; Kim, Y. H., Development of a metal recovery process from Li-ion battery wastes. *Hydrometallurgy* **2005,** *79* (3-4), 172-181.
2. Sole, K. C.; Parker, J.; Cole, P. M.; Mooiman, M. B., Flowsheet options for cobalt recovery in African copper–cobalt hydrometallurgy circuits. *Mineral Processing and Extractive Metallurgy Review* **2018**, 1-13.
3. Olivetti, E. A.; Ceder, G.; Gaustad, G. G.; Fu, X., Lithium-Ion Battery Supply Chain Considerations: Analysis of Potential Bottlenecks in Critical Metals. *Joule* **2017,** *1* (2), 229-243.
4. van der Westhuizen, D. J.; Lachmann, G.; Krieg, H. M. Method for the selective separation and recovery of metal solutes from solution. PCT patent, WO2012168915, 2012.
5. Flett, D. S., Solvent extraction in hydrometallurgy: the role of organophosphorus extractants. *Journal of Organometallic Chemistry* **2005,** *690* (10), 2426-2438.
6. Swartz, B.; Donegan, S.; Amos, A. In *Processing considerations for cobalt recovery from Congolese copperbelt ores*, Hydrometallurgical Conference, The Southern African Institute of Mining and Metallurgy: 2009; pp 385-400.
7. Gabelman, A.; Hwang, S.-T., Hollow fiber membrane contactors. *Journal of Membrane Science* **1999,** *159* (1), 61-106.
8. Parhi, P., Supported liquid membrane principle and its practices: A short review. *Journal of Chemistry* **2012,** *2013*.
9. Neplenbroek, A. M.; Bargeman, D.; Smolders, C., The stability of supported liquid membranes. *Desalination* **1990,** *79* (2-3), 303-312.
10. Pabby, A. K.; Sastre, A. M., State-of-the-art review on hollow fibre contactor technology and membrane-based extraction processes. *Journal of Membrane Science* **2013,** *430*, 263-303.
11. Bacon, I., Solvent extraction as an enabling technology in the nickel industry. *Journal of the Southern African Institute of Mining and Metallurgy* **2002,** *102* (8), 435-443.

CHAPTER 2

Literature survey

2.1) Introduction

Due to increasing demand, depletion of high grade ores, and pressure to recycle, the need for advances in the field of metal recovery, especially from secondary sources, is more important than ever.[1-3] Currently, one metal for which this is particularly true is cobalt (Co). Since the announcement of affordable electrical vehicles (end of 2016), the metal's market price has increased considerably, as shown in Figure 2-1.[4] This price increase can mostly be attributed to the fact that lithium ion batteries (LIBs), which serve as the preferred power source for electrical vehicles, consist of 5 – 20 % Co.[5] Furthermore, the proliferation of portable electronic devices, which also use LIBs, has also played a role in the observed price increase.[6]

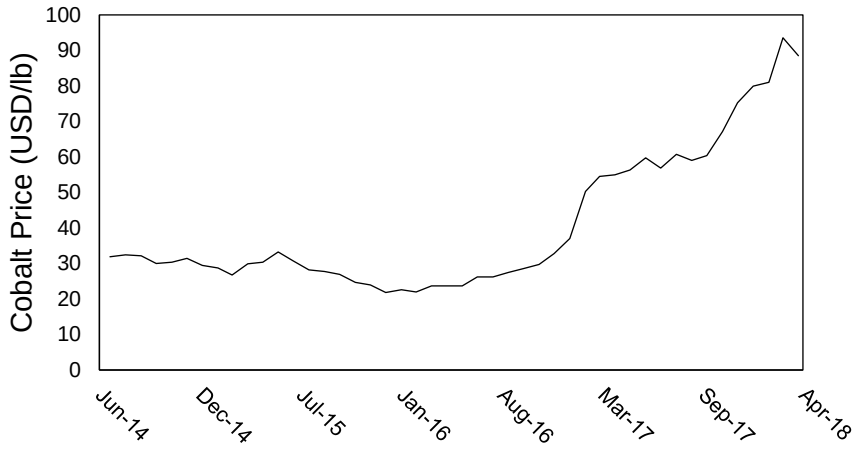

Figure 2-1. Market price of cobalt from June 2014 to April 2018.[4]

Co is generally obtained as a by-product during copper (Cu), nickel (Ni) and zinc (Zn) ore mining, and subsequent processing.[7] The two most important Co deposits are found in the Congolese and Zambian Copperbelt. These deposits are estimated to contain 5.8 and 6.5 million tons of Co, respectively.[8] The Congolese Copperbelt, situated in the Democratic Republic of the Congo (DRC), currently dominates the Co supply. In 2010, the DRC contributed 86 % of the Co mining production in Africa, while accounting for more than 50 % of the world's Co mining production.[9-10] Considering the vast amount of Co available, the supply of Co is not necessarily threatened by diminishing ores, but rather by political instability, geopolitics, corruption, child labour and artisanal mining in the

country that dominates the Co mining production.[11-12] In 1970 for example, the political unrest in the DRC temporarily halted all Co exports, which resulted in a major Co price increase.[11] Additionally, it is not only Co mining that is dominated by a specific country, but also its refining. Co refining is currently predominantly done in China.[11] According to Olivetti et al. (2017), advances in the field of extraction technologies could mitigate the risks associated with the Co supply chain linked to limited suppliers.[11]

It is estimated that 40 % of Co refining in the western hemisphere is achieved using solvent extraction (SX).[7, 13] In fact, SX is one of the major separation and purification unit operations currently used in hydrometallurgy.[14] The success of SX can, at least partially, be attributed to the many highly selective extractants that are commercially available. Additionally, SX can be used to process large volumes of pregnant leach solutions (PLS) produced industrially.[15] However, in order to supply the increasing demand and mitigate the risks associated with the Co supply chain, advances in the field of Co refining are required. This provides the perfect opportunity for the introduction of a novel next generation SX technology, i.e. pertraction (PX), also known as membrane-based solvent extraction.[16]

The focus of this literature study is to provide a background on the hydrometallurgical processing of Co. An overview of conventional hydrometallurgical processes will be given and areas for improvement, with specific emphasis on PX, will be discussed.

2.2) Overview of a generic cobalt processing flowsheet

A generic Co processing flowsheet is presented in Figure 2-2. Co is generally either found as a sulfide or oxide mineral. The most prevalent sulfide mineral is carrolite ($CuCoS_4$), while the most predominant oxide mineral is heterogenite (CoOOH). The flowsheet in Figure 2-2 shows how both Co salt and Co metal product can be obtained from these ores. Generally, Cu, iron (Fe), manganese (Mn), aluminium (Al), magnesium (Mg), calcium (Ca), Zn, and Ni, as well as small amounts of uranium (U), are found as impurities in Co leach solutions.[17] As shown in Figure 2-2, Cu removal is generally done using SX, mainly due to the fact that the technique has lower capital- and operating costs than a precipitation based process.[17-18] Fe, Al and Mn are removed by precipitative oxidation. Fe^{2+} is oxidized to Fe^{3+} and then precipitated as $Fe(OH)_3$ by increasing the pH up to 3.5 using limestone.[17-18] At a pH of 3.5, Al precipitation is enhanced by the presence of phosphate.[17-18] After Fe, Mn and Al removal, U is removed by ion exchange (IX). Secondary Cu removal is done at a pH of 5.5-6.[18], while residual Cu (and small amounts of Zn) and Ni are then removed by cationic IX.[17]

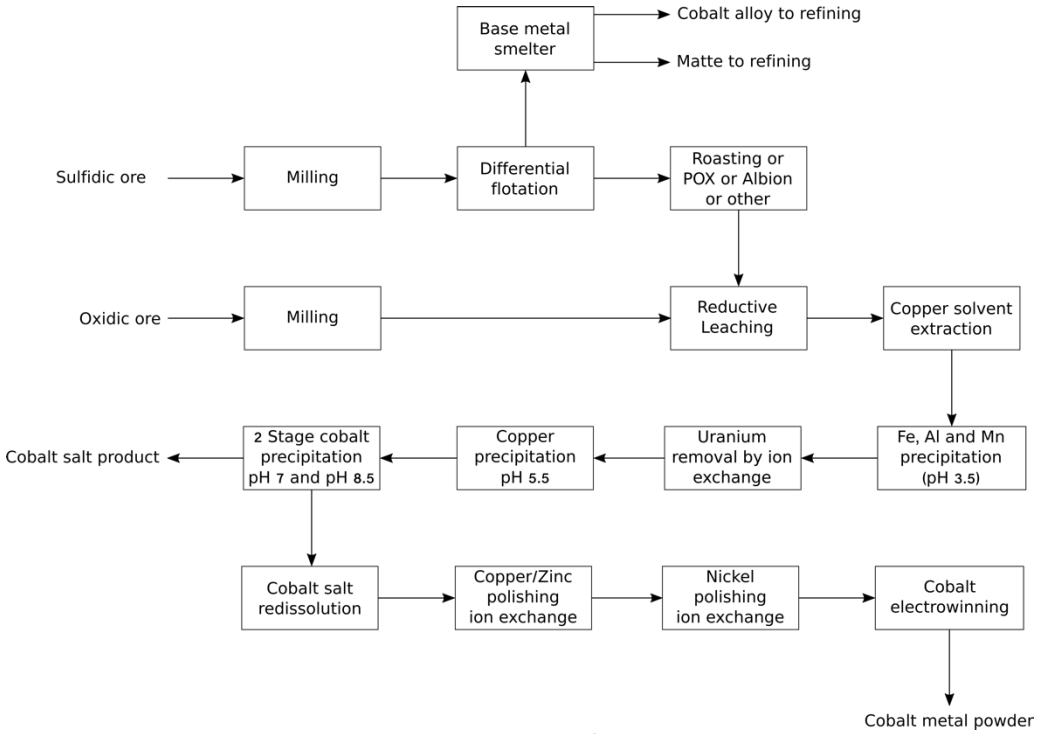

Figure 2-2. Generic cobalt recovery flowsheet.[17-18] POX refers to pressure oxidation.

Ultimately, three cobalt products are suitable for the Co market. These include the hydroxide salt (intermediate product), the carbonate salt (intermediate product) or Co metal.[17] The hydroxide salt, which is the most common Co product, is usually precipitated with either lime (CaO) or magnesia (MgO).[17-18] The obtained product contains either gypsum ($CaSO_4.2H_2O$) or unreacted magnesia.[17-18] The carbonate salt is obtained by means of precipitation using soda ash (Na_2CO_3).[17, 19] In this case, product contaminants include Mn, Ca, and Mg. There are environmental concerns regarding this method due to the use of sodium (Na), which can contaminate water sources.[17] The third Co product, which is the metal, is generally produced via electrowinning (EW).[17] While hydrogen reduction can also be used to produce the metal, EW has lower capital- and operating costs, higher metal yield, requires less stringent operational control and reduced plant maintenance.[17] EW can be operated in one of two ways.[18] The first method includes Co plating in an undivided cell where plating takes place over the full surface of the cathode.[17] The second method uses a divided cell and, in this case, plating is done on screened cathodes, which prevents peeling and bag damage. EW is a purification step in itself as Mn, Ca, Mg and Ni will not plate. Through the use of EW, a metal purity of 99.95 % is achievable. Although the direct metal production has several advantages over the salt production (the metal is cheaper to produce and more valuable than the salts[17]), only one mine (Chambishi metals) in the African Copperbelts produces this product. By atomising the metal to a powder, it can be used as a precursor for any number of desirable Co products.

From a hydrometallurgical point of view, it is logical that a combination of SX and EW should be employed to ultimately process Co. Additionally, the SX processing can be replaced by PX

processing to further optimise the process due to the numerous advantages that PX offers over SX. The ideal hydrometallurgical Co process could therefore be a continuous PX and EW hybrid process.

2.3) Ion-exchange purification of cobalt

IX resins are porous spherical polymeric beads with a typical size of 300 – 1500 μm. The functional groups in IX resins, which are attached to the polymeric matrix, interact selectively with the metal ions in solution. While passing through an IX column, selective adsorption of the metal onto the resin takes place. The adsorption is a reversible reaction and thus regeneration (or elution) of the metal from the resin is possible. Figure 2-3 shows a typical flowsheet where IX unit operations are used to produce a Co advance electrolyte (solution containing 50 g/L Co to be used for Co electrowinning).

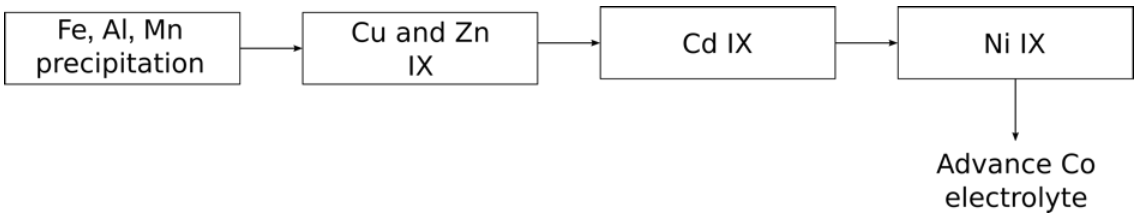

Figure 2-3. Typical flowsheet where ion-exchange unit operations are used to produce an advance Co electrolyte.

From Figure 2-3 it is evident that an IX resin to be used for the removal of Cu and Zn from Co should have a greater affinity for Cu and Zn than for Co to minimize its loading onto the resin. For this, two options are available: imino-diacetic acid resins (IDA) and amino-methyl phosphonic acid resins (AMP). IDA's affinity decreases according to Fe^{3+}> Al^{3+}> Cu^{2+}> Ni^{2+}> Cd^{2+}> Zn^{2+}> Co^{2+}>> Mn^{2+}> Ca^{2+}> Mg^{2+}, while AMP's affinity decreases according to Fe^{3+}> Pb^{2+}> Cu^{2+}> Zn^{2+} Al^{3+}> Ca^{2+}> Ni^{2+}> Co^{2+}> Ca^{2+}> Mg^{2+} Na^{+}.[18, 20] Two resin options also exist for Ni removal, including bis-picolyl-amine (BPA) and hydroxy-propyl-picolylamine (HPPA). Both resins have a higher affinity for Ni than for Co and Co/Ni separation is achieved using split elution. BPA does, however, showcase a high affinity for Cu and, subsequently, a gradual build-up of Cu on the resin occurs over time. This led to the development of HPPA, where Cu can be eluted using H_2SO_4.

Although highly selective resins for Co purification exist, IX resin fouling is a significant industrial problem,[21] especially when dealing with metals such as Fe or Ca. Fe fouling may occur as a result of the deposition of ferric precipitate suspended in the leach liquor or due to precipitation formation (during the process) as a result of Fe^{2+} oxidation in solution.[21] Ca fouling can occur as a result of calcium sulphate precipitation during elution with H_2SO_4.

2.4) Solvent extraction purification of cobalt

Industrially SX has two functions: (i) Solutions purification and (ii) upgrading (concentrating metal in solution). The first use of SX in hydrometallurgy can be dated back to 1942, where ether was used to extract and purify U during the Manhattan project.[22] Since its use in the Manhattan project, SX has become one of the most important purification processes in hydrometallurgy.[22] SX is used globally in numerous applications. Some of these applications include the processing of Cu, Ni, Co, Zn, U, Mo, tungsten (W), vanadium (V), zirconium (Zr), hafnium (Hf), tantalum (Ta), rare earth metals, gallium (Ga), germanium (Ge), platinum group metals (PGMs), to name a few.[22] The success of SX in hydrometallurgical processing can be attributed to the vast amount of selective extractants that are commercially available.

The commercial extractant C272, whose active component is bis(2,4,4-trimethylpentyl)phosphinic acid, shows inimitable selectivity towards Co under optimal experimental conditions. Due to the selectivity of C272, numerous flowsheets have been developed for the recovery of Co from primary and secondary sources.[23-26] Könighofer, et al. [23] developed a method to process Co from copper-cobalt orebodies found in Africa's Copperbelt. The process consists of four extraction stages, two scrubbing stages and three (possibly four) stripping stages. Nogueira and Delmas [24] developed a process in which cadmium (Cd), Co and Ni are separated from one another via two SX circuits. The first circuit uses an organophosphoric acid (D2EHPA) to extract cadmium (Cd) from the feed solution and, during the second circuit, C272 is used for Co extraction. The process developed by these authors can be used to recover the metals from both sulfuric acid leach solutions and spent Ni-Cd batteries.[24] Similarly, Kang, et al. [25] developed a process during which C272 is used to recover Co from spent LIBs, where metal impurities are removed by means of precipitation, followed by the selective extraction of Co using C272.

The success of Co/Ni purification using SX can be attributed to the high selectivity showcased by C272. Co/Ni separation increases in the following order: phosphoric acid < phosphonic acid < phosphinic acid. The structures of these extractants are given in Figure 2-4.[27] The remarkable selectivity for Co by the phosphinic acid can be attributed to the fact that Co forms a stable anhydrous tetrahedral polymeric species in the organic phase whilst Ni remains the hydrated octahedral complex in the aqueous phase.[22, 27] The structure of bis(2,4,4-trimethylpentyl)phosphinic acid, which is commercially sold as C272, can be seen in Figure 2-5. The development of C272 enabled the processing of solutions containing high Ni to Co ratios, i.e. as high as 100:1.[22] According to the specification sheet supplied by Cytec Industries, C272 is currently being used in the majority of Co SX refineries across the globe.

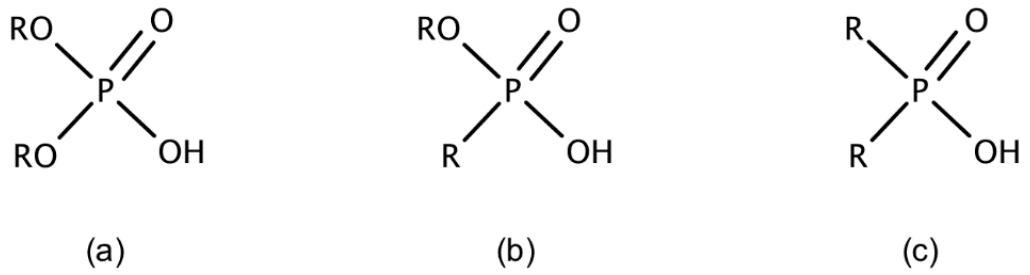

Figure 2-4. Structure of (a) phosphoric, (b) phosphonic and (c) phosphinic acid. The best selectivity for Co is observed with phosphinic acid extractants.

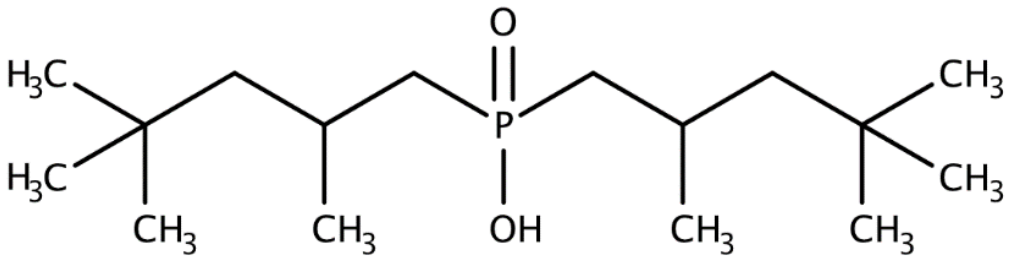

Figure 2-5. Bis(2,4,4-trimethylpentyl)phosphinic acid, commercially sold as Cyanex 272.

The organic extractant can be used to separate Co from Ni from both sulfate and chloride media. From Eq. 1, showing the mechanism by which C272 extracts Co into the organic phase[28], it is evident that the extraction is an equilibrium process during which protons are exchanged for Co ions. As a result, pH control is required to shift the equilibrium of the reaction to obtain optimal extraction. The pH control plays another role in that it is used to increase the Co/Ni separation as Ni co-extracts at pH values ≥ 5.5.[23, 29] The pH of the aqueous phase can be regulated by buffering or by continuously adding a base, such as NaOH, to the solution.[17, 28]

$$Co^{2+}_{Aq} + 2(HR)_{Org} \rightleftharpoons CoR_{2,Org} + 2H^{+} \quad (1)$$

An alternative pH control method is the pre-neutralisation of C272, which can be done using bases such as sodium hydroxide, Na_2CO_3 and ammonium hydroxide.[30] An example of a pre-neutralisation reaction using sodium hydroxide is given in Eq. 2, whereas the overall extraction reaction, using pre-neutralised C272, is given in Eq. 3.[28, 30]

$$2NaOH_{Aq} + (HR)_{2,\,Org} \rightleftharpoons 2NaR_{Org} + 2H_2O_{Aq} \quad (2)$$

$$Co^{2+}_{Aq} + 2NaR_{\,Org} \rightleftharpoons CoR_{2,Org} + 2Na^{+} \quad (3)$$

From Eq. 3, it is evident that the extraction using pre-neutralised C272 does not involve proton generation. Subsequently, pre-neutralisation enables a “pH-neutral” extraction reaction where similar results are obtained compared to those when using continuous pH control.[30] The use of pre-neutralisation offers numerous advantages over mixbox pH control (base is directly added to the emulsion in the mixer). Mixbox pH control requires the removal of a portion of the aqueous phase from the mixbox emulsion in order to obtain an accurate pH measurement.[30] This extra step requires additional equipment and the pH electrode requires regular maintenance and calibration to prevent organic fouling and scaling.[30] Furthermore, the addition of a base directly into the mixer can cause pH spikes in certain regions of the mixer which, subsequently, lead to the formation of metal hydroxide precipitates within the mixer.[30] To prohibit the formation of these metal hydroxide precipitates, the use of a dilute base is required, which negatively affects the water balance.[30]

Although numerous methods are used for the purification of Co, such as selective crystallization/precipitation, IX, adsorption with chelating ion exchange resins, and chromatography, SX is one of the most versatile techniques to process Co from mixed metal aqueous solutions.[29, 31-33] Due to the versatility of SX processing, numerous SX flowsheets have been developed to refine Co from primary, as well as secondary sources. A typical flowsheet for the hydrometallurgical processing of mixed metal aqueous solutions using SX for solution purification and upgrading is shown in Figure 2-6.[1, 23, 29] Product specifications are achieved using numerous extraction and scrubbing stages, where additional scrubbing stages can be added to obtain the target purity. Generally, during Co SX, co-extracted Ni is scrubbed using a small amount of the advance electrolyte, which is circulated back to the extraction section after scrubbing.

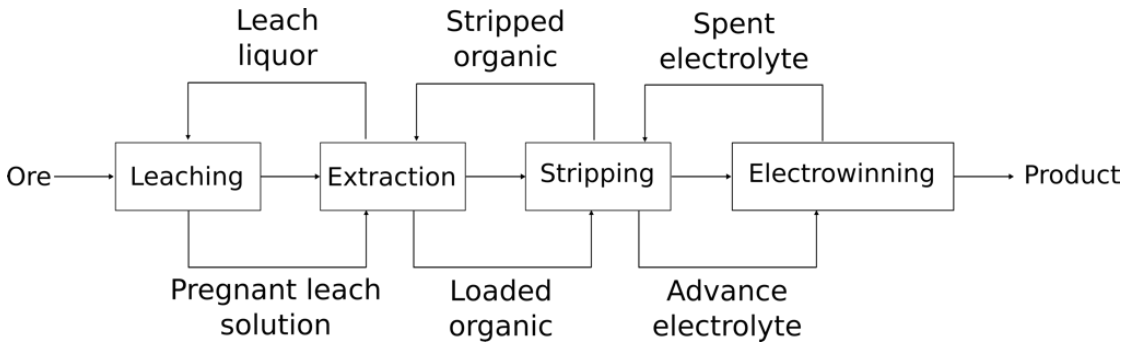

Figure 2-6. Typical flowsheet for the hydrometallurgical processing of mixed metal aqueous solutions where solvent extraction unit operations are used for the purification and upgrading of the advance electrolyte solution for direct metal production.

The use of SX together with C272 for the recovery and purification of Co and Ni is well documented and the technique has been the industrial workhorse for this application for decades.[28] The technique does still, however, have numerous disadvantages. Some of these disadvantages include foaming, flooding, unloading, stable emulsion formation and the need for density differences.[34] Due to the fact

that membrane-based SX is a non-dispersive technique, many of the disadvantages associated with SX can be overcome by using this technique.[34]

2.5) Pertraction purification of cobalt

PX, also referred to as membrane-based SX, is a combination of SX and membrane technology where the membrane acts as a semipermeable barrier between the aqueous- and organic phase. Phase entrainment is prohibited by applying a slight overpressure on the non-wetting liquid side of the module.[35] The major disadvantage of PX, relative to SX, is the possibility of membrane fouling which can lead to significant operational costs attributed to membrane cleaning or replacement. Additionally, the membrane material has to be stable in the specific chemical environment to be used in the processing of materials. PX does, however, offer numerous industrial advantages over conventional SX, as listed below.

- The phases are not mixed and consequently no settlers are required, reducing plant size and cost.
- The metal lock-up in the plant is reduced.
- Less rotating equipment is required, leading to a reduction in maintenance costs.
- Significant process intensification.
- Straightforward process design.
- PX is considerably safer than SX since it is a closed system.

Even though there are numerous challenges involved with the implementation of a new technology industrially, improvements are nevertheless required in the field of separation technology.[35] One area where PX has already been applied successfully is in the removal of hydrophobic organic compounds from water streams.[35] Accordingly, PX can be used to treat waste water streams containing aromatic and aliphatic organic compounds, chlorinated solvents, polychlorinated biphenyls, di- and trichlorobenzene, pesticides and higher polycyclic hydrocarbons.[35] In 1998 KoSa BV, a company situated in the Netherlands, successfully implemented a PX process to treat contaminated water originating from one of their chemical reactors.[35] The process uses Liqui-Cel™ membrane contactors to treat waste water that is heavily polluted with the product formed in the reactor (an aromatic compound).[35] Additionally, the pollutant is extracted into the feedstock for the reactor.[35] Subsequently, the waste water is not only treated but product losses are also reduced.[35]

Verbeken, et al. [36] showed that a synergistic extractant (LIX 860-I and D2EHPA) could be used to recover Co from dilute solutions using PX on a pilot-scale. In a particularly interesting PX application, Yang and Kocherginsky [37] investigated the recovery of Cu from spent ammoniacal etching solutions.

During the production of printed circuit boards, ammoniacal etching solutions are used for the etching of a thin layer of Cu. After etching, the spent solutions can contain up to 1 g Cu/L. The authors used a 1.4 m^2 bench-scale setup to optimise the process, after which a 130 m^2 pilot-scale study was perfomed.[37] The results obtained during the pilot-scale study were promising for future industrial implementation.[36]

Models that are suitable both for the interpretation of batch PX results and the conceptual design of a continuous PX plant are given in Table 2-1. For the mass transfer, a typical first-order diffusion model through a porous membrane with the concentration difference as driving force was used.[38] However, as the overall mass transfer coefficient also depends on the raffinate concentration via the distribution coefficient (D_M), PX is not necessarily a first-order process. The resistance-in-series module has been investigated by various authors.[39-40] The main difference between these studies and previous research on these models is the large increase in the distribution of Co (D_{Co}) between the start and the end of the batch run (or the feed and the raffinate side of the continuous process), resulting in an increase in the mass transfer coefficient. This is taken into account in the modelling process. As it is difficult to distinguish between the mass transfer resistance of the solvent in the pores ($1/k_M$) and in the lumen ($1/k_{Org}$), both are added as $1/k_{MO}$, where $1/k_{ov} = 1/k_{Aq} + 1/Dk_{MO}$.

The solvent-to-feed ratio was taken as 1.2 multiplied by the minimum value, which was taken as the ratio of the feed concentration over the solvent equilibrium concentration, i.e. $1/D_F$. The total pressure drop was calculated by adding the pressure drop over both circuits and the overpressure applied on the aqueous phase (to prevent phase entrainment). The total pressure drop should be smaller than the bubble pressure of the membrane to prevent breakthrough of the aqueous phase into the organic phase. Since the solvent viscosity is proportional to the pressure drop and inversely proportional to the mass transfer, the viscosity is an important parameter in the conceptual design process of a PX plant. To calculate the solvent viscosities, the Kendall-Monroe model can be used, as has been shown by Koekemoer, et al. [41]

Table 2-1. Comprehensive set of pertraction models.

Model	Batch PX	Continuous PX
Mass transfer	$\frac{dx}{dt} = -\frac{k_{ov}A}{V_{aq}}\left(x - \frac{y}{D}\right)$	$\frac{dx}{dL} = -\frac{k_{ov}A}{Q_{Aq}}\left(x - \frac{y}{D}\right)$
Resistance-in-series	$\frac{1}{k_{ov}} = \frac{1}{k_{aq}} + \frac{1}{Dk_M} + \frac{1}{Dk_{org}} = \frac{1}{k_{aq}} + \frac{1}{Dk_{Mo}}$	
Mass balance	$V_{aq}\frac{dx}{dt} + V_{org}\frac{dy}{dt} = 0$	$Q_{Aq}\frac{dx}{dL} = Q_{Org}\frac{dy}{dL}$
Isotherm	$y = f(x); D = \frac{y}{x}$	
Solvent-to-feed ratio	$\frac{V_{org}}{V_{aq}} = \frac{1.2}{D_F}$	$\frac{Q_{Org}}{Q_{Aq}} = \frac{1.2}{D_F}$
Pressure drop constraint	$\Delta p_{total} \leq \Delta p_{bubble}$	
Solvent viscosity (Kendall–Monroe)	$\mu_o = \left(\sum_i \hat{z}_i \mu_i^{1/3}\right)^3$	

From the above-mentioned it is clear that a conceptual design for a PX refinery plant can be made using data relating to the feed composition, mass balance, isotherms and mass transfer kinetics in conjunction with the process models given in Table 2-1.

2.6) Electrowinning of Co

After solution purification and upgrading via SX, EW is generally used for the production (and further purification) of metallic Co. Typical London Metal Exchange (LME) specifications for Co metal are listed in Table 2-2 and a simplified flowsheet for cobalt metal production (from African Copperbelt orebodies) is given in Figure 2-7. The cathodic and anodic reactions (together with their standard reduction potential) that take place during Co EW are given in Eq. 4 and Eq. 5, respectively. From the overall reduction potential of - 1.51 V vs SHE, we can see that the reaction is not spontaneous. Additionally, due to the applied overpotential H_2 evolution (Eq. 6) competes with Co plating on the cathode. Although hydrogen evolution is the thermodynamically preferred reaction, it can be avoided through the use of divided cells, high Co concentration in the advance electrolyte, temperature control and high current densities.

$$Co^{2+} + 2e^- \longrightarrow Co \qquad E^0 = -0.28\ V \qquad (4)$$

$$2H_2O \longrightarrow O_2 + 4H^+ + 2e^- \qquad E^0 = -1.23\ V \qquad (5)$$

$$2H^{2+} + 2e^- \longrightarrow H_2 \qquad E^0 = 0\ V \qquad (6)$$

Table 2-2. Typical London Metal Exchange specifications for cobalt.[18]

Element	Specification
Co	> 98.8 %
Cu	< 200 ppm
Fe	< 2000 ppm
Mn	< 1000 ppm
Ni	< 5500 ppm
Ca	< 250 ppm
Mg	< 250 ppm
Cd	< 100 ppm
Pb	< 100 ppm
Zn	< 500 ppm
S	< 500 ppm
C	< 500 ppm

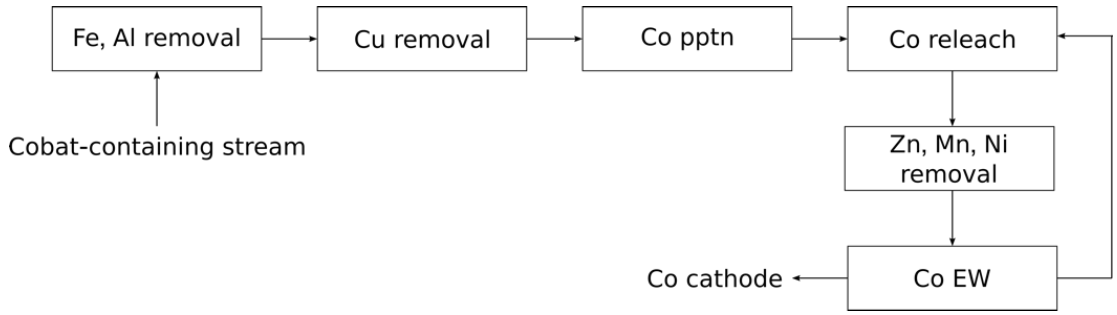

Figure 2-7. Simplified flowsheet for cobalt metal production as generally done on the African Copperbelt. Pptn refers to precipitation.

One of the major concerns during Co metal production is the quality of plating (brittleness and internal stress), which is affected by pH, temperature, current density and electrolyte purity.[42] High acidity can lead to high hydrogen evolution which causes low current efficiency. Additionally, hydrogen can be incorporated into the metal which leads to embrittlement of the metal. On the other hand, low temperature can cause a decrease in the electrolyte conductivity, which results in high cell voltage and increased power consumption. Low temperatures also cause an increased rate of H_2 evolution competing with the Co reduction. While an increased current density has a small effect on current efficiency, it enhances the morphology and thickness of the deposit. High Co concentrations in the advance electrolyte improve the plating quality due to the fact that it increases the Co to proton ratio by replenishing Co^{2+} at the plating surface.

The major impurities of concern during EW of Co include Cu, Zn, Fe, Mn and Ni. The cathodic half reactions of these metals are given in Table 2-3, together with their respective standard reduction potentials. As expected, any Cu in the advance Co electrolyte will co-plate on the cathode and subsequently contaminate the Co metal product. Although it is not theoretically expected that Zn will co-deposit on the cathode (see Table 2-3), this anomalous deposition has been observed in practice.[43] The anomalous deposition of Fe is also observed in practice.[43-44] Although Mn will not compete with Co deposition on the cathode, it is known to deposit as MnO_2 on the anode, leading to lead contamination due to the breakdown of the lead anode.[17, 44] Finally, it is expected that, thermodynamically, Ni would plate preferentially over Co. In practice, however, the Co to Ni ratio in the deposit is approximately 5 to 10 times higher than that of the electrolyte.

Table 2-3. Cathodic half reactions of common impurities associated with Co EW.

Cathodic half reaction	E^0 vs SHE (V)
$Co^{2+} + 2e^- \longrightarrow Co$	-0.28
$Cu^{2+} + 2e^- \longrightarrow Cu$	0.34
$Zn^{2+} + 2e^- \longrightarrow Zn$	-0.76
$Fe^{3+} + e^- \longrightarrow Fe^{2+}$	0.77
$Mn^{2+} + 2e^- \longrightarrow Mn$	-1.18
$Ni^{2+} + 2e^- \longrightarrow Ni$	-0.26

In conclusion, when using an electrolyte purified and upgraded to ≥ 50 g/L Co (advance electrolyte), EW can produce Co metal of a purity of 99.95 %, which is well within the LME specifications. Hydrogen evolution and plating quality can be controlled through the use of optimal parameters such as pH, temperature, current density and electrolyte purity. Additionally, the use of divided cells with the incorporation of membrane technology should also be considered to mitigate the concerns associated with traditional Co EW. Although the direct EW of metallic Co was not attempted during this study, the requirements of an advance electrolyte served as the target specifications due to the fact that EW is the last step in metallic Co productions.

2.7) Conclusion

From the detailed discussions of various processing techniques, it is evident that SX is a workhorse in Co processing. It is a well-documented technique that is evidently used in the majority of Co processing plants. The success of SX in the processing of Co can be attributed to the inimitable selectivity of the commercial extractant C272 towards Co. Despite the success that SX has shown in the processing of Co, the technique does, however, have numerous disadvantages, which can majorly be attributed to the fact that the technique requires mixing of the organic and aqueous phases, leading, for example, to flooding and emulsion formations.

Since PX entails the use of a membrane, thereby avoiding the mixing of the phases, many of the disadvantages regarding SX can be overcome. Additional industrial advantages that PX offer over SX include process intensification, reduced plant size, reduced maintenance costs and increased safety. Furthermore, a set of comprehensive models were identified for the straightforward conceptual design of the extraction section of a PX processing plant.

Despite the challenges involved when introducing a new technology industrially, improvements in the field of separation technology are nonetheless required to supply the increasing demand while mitigating the risks associated with the Co supply chain. These requirements create the perfect opportunity for the introduction of the next generation SX, i.e. PX.

2.8) References

1. Wilson, A. M.; Bailey, P. J.; Tasker, P. A.; Turkington, J. R.; Grant, R. A.; Love, J. B., Solvent extraction: the coordination chemistry behind extractive metallurgy. *Chem Soc Rev* **2014,** *43* (1), 123-34.
2. Gramatyka, P.; Nowosielski, R.; Sakiewicz, P., Recycling of waste electrical and electronic equipment. *Journal of Achievements in Materials and Manufacturing Engineering* **2007,** *20* (1-2), 535-538.
3. Graedel, T. E.; Allwood, J.; Birat, J. P.; Buchert, M.; Hagelüken, C.; Reck, B. K.; Sibley, S. F.; Sonnemann, G., What do we know about metal recycling rates? *Journal of Industrial Ecology* **2011,** *15* (3), 355-366.
4. Anon. Cobalt Futures. https://www.investing.com/commodities/cobalt-historical-data (accessed 31 March 2018).
5. Shin, S. M.; Kim, N. H.; Sohn, J. S.; Yang, D. H.; Kim, Y. H., Development of a metal recovery process from Li-ion battery wastes. *Hydrometallurgy* **2005,** *79* (3-4), 172-181.
6. Li, J.; Shi, P.; Wang, Z.; Chen, Y.; Chang, C. C., A combined recovery process of metals in spent lithium-ion batteries. *Chemosphere* **2009,** *77* (8), 1132-6.
7. Sharma, I.; Alex, P.; Bidaye, A.; Suri, A., Electrowinning of cobalt from sulphate solutions. *Hydrometallurgy* **2005,** *80* (1-2), 132-138.
8. Hitzman, M.; Broughton, D.; Selley, D.; Woodhead, J.; Wood, D.; Bull, S., *The Central African Copperbelt: Diverse stratigraphic, structural and temporal settings the world's largest sedimentary copper district*. 2012; Vol. 16, p 487-514.
9. Yager, T. R.; Bermudez-Lugo, O.; Mobbs, P. M.; Newman, H. R.; Taib, M.; Wallace, G. J.; Wilburn, D. R., The Mineral Industries of Africa. *US Geological Survey US Geological Survey (USGS)[Электронный ресурс]. URL: http://minerals. er. usgs. gov* **2010**.
10. Nansai, K.; Nakajima, K.; Kagawa, S.; Kondo, Y.; Suh, S.; Shigetomi, Y.; Oshita, Y., Global flows of critical metals necessary for low-carbon technologies: the case of neodymium, cobalt, and platinum. *Environ Sci Technol* **2014,** *48* (3), 1391-400.
11. Olivetti, E. A.; Ceder, G.; Gaustad, G. G.; Fu, X., Lithium-Ion Battery Supply Chain Considerations: Analysis of Potential Bottlenecks in Critical Metals. *Joule* **2017,** *1* (2), 229-243.
12. Smith, L. Cobalt Controversies: Delving into the How, What and Why 2017. https://www.coreconsultantsgroup.com/cobalt-controversies/.
13. Ayanda, O.; Adekola, F.; Baba, A.; Fatoki, O., *Application of Cyanex® Extractant in Cobalt/Nickel Separation Process by Solvent Extraction*. 2013; Vol. 8.
14. Othman, N.; Goto, M.; Mat, H., Liquid Membrane Technology For Precious Metals Recovery From Industrial Waste. In *Regional Symposium on Membrane Science and Technology*, Johor, Malaysia, 2018.
15. Xie, F.; Zhang, T. A.; Dreisinger, D.; Doyle, F., A critical review on solvent extraction of rare earths from aqueous solutions. *Minerals Engineering* **2014,** *56*, 10-28.
16. van der Westhuizen, D. J.; Lachmann, G.; Krieg, H. M. Method for the selective separation and recovery of metal solutes from solution. PCT patent, WO2012168915, 2012.
17. Swartz, B.; Donegan, S.; Amos, A. In *Processing considerations for cobalt recovery from Congolese copperbelt ores*, Hydrometallurgical Conference, The Southern African Institute of Mining and Metallurgy: 2009; pp 385-400.
18. Sole, K. C.; Parker, J.; Cole, P. M.; Mooiman, M. B., Flowsheet options for cobalt recovery in African copper–cobalt hydrometallurgy circuits. *Mineral Processing and Extractive Metallurgy Review* **2018**, 1-13.
19. Boyton, R. S., *Chemistry and Technology of Lime and Limestone*. Second ed.; John Wiley & Sons: New York, 1980.
20. Sole, K.; Jurrius, Y.; Hardwick, E., *Purification of a cobalt electrolyte by ion exchange: pilot-plant results and preliminary commercial design*. 2016.
21. Duke, H.; Featherstone, J. L.; Marston, C. R. METHOD FOR CLEANING FOULED ON EXCHANGE RESINS. US6080696A, 2000.
22. Flett, D. S., Solvent extraction in hydrometallurgy: the role of organophosphorus extractants. *Journal of Organometallic Chemistry* **2005,** *690* (10), 2426-2438.

23. Könighofer, T.; Archer, S.; Bradford, L., A cobalt solvent extraction investigation in Africa's Copper Belt. *Journal of the Southern African Institute of Mining and Metallurgy* **2009,** *109* (6), 337-342.
24. Nogueira, C. A.; Delmas, F., New flowsheet for the recovery of cadmium, cobalt and nickel from spent Ni–Cd batteries by solvent extraction. *Hydrometallurgy* **1999,** *52* (3), 267-287.
25. Kang, J.; Senanayake, G.; Sohn, J.; Shin, S. M., Recovery of cobalt sulfate from spent lithium ion batteries by reductive leaching and solvent extraction with Cyanex 272. *Hydrometallurgy* **2010,** *100* (3), 168-171.
26. Feather, A.; Bouwer, W.; Swarts, A.; Nagel, V., Pilot-plant solvent extraction of cobalt and nickel for Avmin's Nkomati project. *JOURNAL-SOUTH AFRICAN INSTITUTE OF MINING AND METALLURGY* **2002,** *102* (8), 457-462.
27. Sarangi, K.; Reddy, B.; Das, R., Extraction studies of cobalt (II) and nickel (II) from chloride solutions using Na-Cyanex 272.: Separation of Co (II)/Ni (II) by the sodium salts of D2EHPA, PC88A and Cyanex 272 and their mixtures. *Hydrometallurgy* **1999,** *52* (3), 253-265.
28. Hereijgers, J.; Vandermeersch, T.; Van Oeteren, N.; Verelst, H.; Song, H.; Cabooter, D.; Breugelmans, T.; De Malsche, W., Separation of Co(II)/Ni(II) with Cyanex 272 using a flat membrane microcontactor: Extraction kinetics study. *Journal of Membrane Science* **2016,** *499*, 370-378.
29. Swain, B.; Cho, S.-S.; Lee, G. H.; Lee, C. G.; Uhm, S., Extraction/separation of cobalt by solvent extraction: a review. *Applied Chemistry for Engineering* **2015,** *26* (6), 631-639.
30. Szolga, W. In *Flowsheet Developments using Cyanex reagents*, ALTA, Perth, Australia, 20-27 May; Perth, Australia, 2017.
31. Kholmogorov, A. G.; Kononova, O. N.; Patrushev, V. V.; Mikhlina, E. V.; Kononov, Y. S.; Pashkov, G. L., Ion exchange purification of manganese sulphate solutions from cobalt. *Hydrometallurgy* **1997,** *45* (3), 261-269.
32. Mendes, F. D.; Martins, A. H., Recovery of nickel and cobalt from acid leach pulp by ion exchange using chelating resin. *Minerals Engineering* **2005,** *18* (9), 945-954.
33. Sevenich, G. J.; Fritz, J. S., Addition of complexing agents in ion chromatography for separation of polyvalent metal ions. *Analytical Chemistry* **1983,** *55* (1), 12-16.
34. Gabelman, A.; Hwang, S.-T., Hollow fiber membrane contactors. *Journal of Membrane Science* **1999,** *159* (1), 61-106.
35. Pabby, A. K.; Sastre, A. M., State-of-the-art review on hollow fibre contactor technology and membrane-based extraction processes. *Journal of Membrane Science* **2013,** *430*, 263-303.
36. Verbeken, K.; Vanheule, B.; Pinoy, L.; Verhaege, M., Cobalt removal from waste-water by means of supported liquid membranes. *Journal of Chemical Technology & Biotechnology* **2009,** *84* (5), 711-715.
37. Yang, Q.; Kocherginsky, N. M., Copper recovery and spent ammoniacal etchant regeneration based on hollow fiber supported liquid membrane technology: From bench-scale to pilot-scale tests. *Journal of Membrane Science* **2006,** *286* (1-2), 301-309.
38. Mulder, J., *Basic Principles of Membrane Technology*. Springer Netherlands: 2012.
39. Baudot, A.; Floury, J.; Smorenburg, H. E., Liquid-liquid extraction of aroma compounds with hollow fiber contactor. *AIChE journal* **2001,** *47* (8), 1780-1793.
40. Sengupta, A.; Peterson, P. A.; Miller, B. D.; Schneider, J.; Fulk, C. W., Large-scale application of membrane contactors for gas transfer from or to ultrapure water. *Separation and Purification Technology* **1998,** *14* (1), 189-200.
41. Koekemoer, L. R.; Badenhorst, M. J. G.; Everson, R. C., Determination of Viscosity and Density of Di-(2-ethylhexyl) Phosphoric Acid + Aliphatic Kerosene. *Journal of Chemical & Engineering Data* **2005,** *50* (2), 587-590.
42. Lupi, C.; Pilone, D., Electrodeposition of nickel-cobalt alloys: the effect of process parameters on energy consumption. *Minerals Engineering* **2001,** *14* (11), 1403-1410.
43. Kongolo, K.; Mutale, C.; Kalenga, M., Contribution of nickel, zinc and sulphur co-deposistion during cobalt electrowinning. *Journal-South African Institute of Mining and Metallurgy* **2005,** *105* (9), 599.
44. Mulaudzi, N.; Kotze, M. In *Direct cobalt electrowinning as an alternative to intermediate cobalt mixed hydroxide product*, Base Metals Conference. The Southern African Institute of Mining and Metallurgy. Johannesburg, 2013; pp 209-222.

CHAPTER 3

MATERIALS AND METHODS

3.1) Materials and liquid phase preparation

3.1.1) Aqueous solution preparation

3.1.1.1) Synthetic

Synthetic feed solutions were prepared by dissolving the appropriate amount of cobalt(ii) sulfate heptahydrate ($CoSO_4.7H_2O$) and nickel(ii) sulfate hexahydrate ($NiSO_4.6H_2O$) in deionised water (Millipore Milli-Q Plus® Q-pack CPMQ004R1), which was also used in all other aqueous dilutions in this study. The cobalt (Co) concertation was varied between 1 and 4 g/L throughout the study, whilst the nickel (Ni) concentration was kept constant at 10 g/L (unless noted otherwise). The pH of the aqueous solutions was controlled using ammonium hydroxide (NH_4OH) or sulfuric acid (H_2SO_4). Specifications of the reagents used to prepare the synthetic aqueous feed solutions are given in Table 3-1.

Table 3-1. Specifications of reagents used to prepare aqueous solutions. The low purity of Co and Ni salts arises from the hygroscopic nature of the salts.

Reagent (purity)	Supplier
$CoSO_4.7H_2O$ (≥ 90 %)	Anyang General Chemical Co.,Ltd
$NiSO_4.6H_2O$ (≥ 95 %)	Anyang General Chemical Co.,Ltd
Ammonium hydroxide (25 %)	Minema
Sulfuric acid (≥ 98 %)	LABCHEM

3.1.1.2) Industrial pregnant leach solution

As mentioned previously, both simulated and real solutions obtained from Minemet PTY(LTD) were used in this study. The Co, Ni, iron (Fe), manganese (Mn) and molybdenum (Mo) contents in the pregnant leach solution (PLS) supplied by Minemet PTY(LTD), after the processing described in Chapter 1, are presented in Table 3-2.

Table 3-2. Chemical composition of the PLS supplied by Minemet PTY(LTD).

Metal	Concentration (g/L)
Co	4.61
Ni	10.73
Fe	0.03
Mn	0.17
Mo	0.12

3.1.2) Solvent preparation

To the required amount of Cyanex 272 (C272) organic reagent (i) NH_4OH (pre-neutraliser), (ii) 5 %(v/v) 1-octanol (modifier) and (iii) a small amount Shellsol 2325 (diluent) was added. The modifier was added in order to prohibit the formation of emulsions and improve phase separation. When NH_4OH is added to the solvent, the NH_4^+ ion replaces the ionisable proton on the C272 extractant. This process is known as pre-neutralisation. The mixture was stirred and allowed to stand until all the components had dissolved. After complete dissolution of the solvent components, the mixture was diluted to the appropriate volume using Shellsol 2325. The specifications of the reagents used for solvent preparation are presented in Table 3-3.

Table 3-3. Specifications of reagents used to prepare solvent solutions.

Reagent (purity)	Supplier
Cyanex 272 (85 %)	Solvay
Ammonium hydroxide (25 %)	Minema
1-octanol (> 98 %)	Fisher Scientific
Shellsol 2325	CHEMQUEST AFRICA

3.2) Liquid-liquid extraction

Solvent extraction (SX) experiments were performed by contacting the aqueous and organic phases in a volume ratio of 1:1 (unless noted otherwise). Agitation proceeded for 60 min. to ensure that the extraction reaction reached equilibrium. A shaking incubator was used for agitation at 25 $\pm$ 2.5 ºC and 300 rpm. After contact, the phases were separated using separation funnels. The aqueous solution was analysed both before and after extraction using ICP-OES (Agilent 5110), while the metal concentrations in the organic phases were calculated using mass balances.

The ICP-OES instrument was calibrated by preparing standards (99.999 %, De Bruyn spectroscopic solutions) in the required range for each experiment and the experimental samples were diluted to

align with the calibration range, taking into account the detection and saturation limits of the ICP-OES. For each calibration run a quality control (QC) was introduced made from a secondary standard source (99.999 %, De Bruyn spectroscopic solutions) to ensure accuracy and verification of the calibration line. With the being sampled for calibration verification after 10 samples were analysed, as well as the QC being determined at the end of each run.

From the liquid-liquid extraction (LLE) experiments, extraction, scrubbing and stripping data was obtained. By repeating numerous experimental data points, an experimental error for the LLE data was found to be < 6.2 %. The error was calculated by determining the standard deviation and subsequently converting this to a percentage value relative to the average of the repeated data points.

3.2.1) Extraction

3.2.1.1) pH curves

Extraction as a function of pH was determined using the same general SX procedure described previously. The feed pH values were varied using H_2SO_4 or NH_4OH.[1] pH measurements of the feed (pH_{Feed}) and raffinate ($pH_{Equilibrium}$) were performed using a Metrohm 744 pH meter with a 6.0258.010 electrode. The pH meter was calibrated, before each series of sample analysis, using pH 4.01 and 7.01 buffer solutions (Hanna instruments). The calibration was repeated in the case where the calibration line was below 95 %, with KCl electrolyte being refreshed when the calibration lowered below acceptable levels. Additionally, calibration verification was performed using a separate QC, i.e. pH 4.00 buffer solution (C.C. Imelmann PTY(LTD)).

3.2.1.2) Distribution isotherms

The extraction isotherms of pure Co solutions (≥ 90 %, Anyang General Chemical Co.,Ltd) were determined in the range 0.01-10 g/L Co for three different C272 extractant concentrations (9; 15 and 22 wt%). The feed pH was kept constant at values between 5.0 and 5.5 by using NH_4OH. The lower value of 0.01 g/L Co corresponds to a Ni purity of 99.9 % (in the raffinate) from a PLS containing 10 g/L Ni (feed). For an adequate design of the PX column, it is important to know the shape of the isotherm in the raffinate region, thus significant effort was made to obtain data in the 0.01 g/L Co range.

3.2.2) Scrubbing

A 50 g/L Co scrubbing solution was prepared using $CoSO_4.7H_2O$ (≥ 98 %, Minema). The scrubbing solution was contacted with a loaded solvent. The loaded solvent was prepared by contacting a 22 wt% C272 solvent with an industrial PLS supplied by Minemet PTY(LTD) containing 4.70 g/L Co

and 10.85 g/L Ni. The composition of the loaded solvent was determined using ICP-OES analyses of the feed and raffinate in conjunction with mass balance. The scrub solution was contacted using various volume ratios and pH values. The organic to aqueous (O/A) ratios included 30, 40 and 50, while the pH values were varied between 4.0 and 5.0.

3.2.3) Stripping

Since Co electrowinning (EW) is usually done in H_2SO_4 solutions, the stripping efficiency of H_2SO_4 stripping liquors were considered in the range of 0.0 – 0.3 M H_2SO_4. The liquors were prepared by diluting the appropriate amount of H_2SO_4 using deionised water. After preparation of the stripping liquors, they were contacted with 22 wt% C272 solvents loaded with 1.08 g/L Co and 11.26 g/L Ni according to the general SX procedure discussed previously.

The stripping isotherms of two stripping liquors, 0.1 and 0.2 M H_2SO_4, were determined. The loaded solvents, in the range 1.11 - 6.67 g/L Co, were prepared by contacting feed samples with a 22 wt% C272 solvent prepared according to the general procedure (Section 3.2). Feed solutions, in the range of 1.11 – 11.13 g/L Co, were prepared by dissolving the appropriate amount of $CoSO_4.7H_2O$ ($\geq$ 98 %, Minema) in deionised water, followed by pH adjustments to values between 5.0 and 5.5. Feed and solvent samples were contacted with an A/O ratio of 1:1 at 25 $\pm$ 2.5 ºC and 300 rpm for 60 min using a shaking incubator. After contact, the loaded solvents were separated from the raffinates and used to determine the stripping isotherms of the strip liquors. For both the 0.1 and 0.2 M H_2SO_4 strip liquors, aqueous and organic phases were contacted in O/A ratios of 1:1 at 25 $\pm$ 2.5 ºC and 300 rpm using a shaking incubator until equilibrium had been reached.

3.3) Batch pertraction

In this study, a 3M™ Liqui-Cel™ EXF-2.5x8 module was used for the pertraction (PX) experiments. A schematic representation of the module is given in Figure 3-1.[2] The module is a hydrophobic hollow fiber membrane contactor, implying that the organic phase can permeate the membrane whilst the aqueous phase cannot. However, breakthrough of the organic phase is easily prohibited by applying a small overpressure on the aqueous side. The feed can either be fed through the shell (area surrounding membrane fibers) or lumen (area inside the fibers). Table 3-4 shows the dimensions and flow conditions of the module.[3] The module, with a diameter of 6.25 cm and a length of 20 cm, delivers a contact area of 1.4 m^2, resulting in significant process intensification. As seen in Figure 3-1, the module contains a baffle which enables cross flow. Due to the baffle, the fluid in the shell side flows not only in the opposite direction, but also perpendicularly to the fluid in the lumen side, which promotes turbulence in the shell side and, subsequently, enhances mass transfer outside the fibres.[4]

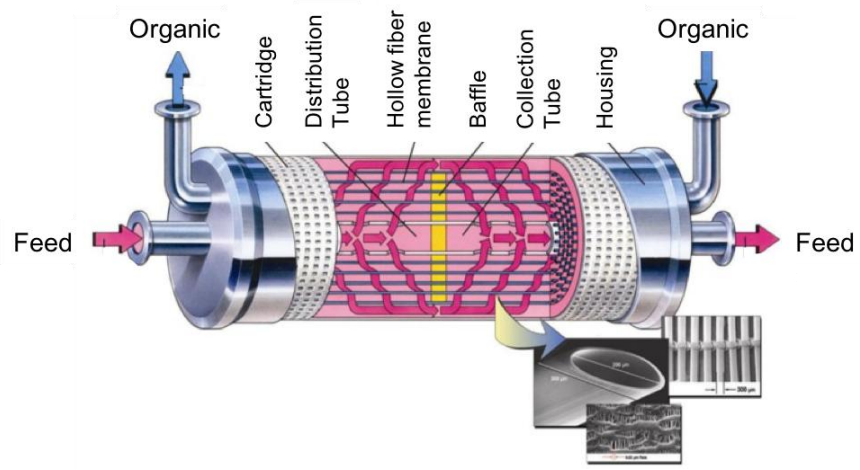

Figure 3-1. Schematic representation of the 3M™ Liqui-Cel™ EXF-2.5x8 series membrane contactor with a contact area of 1.4 m^2.[2]

Table 3-4. Dimensions and flow conditions of the 3M™ Liqui-Cel™ EXF-2.5x8 module.[3]

Dimension	Value	Unit of measurement
Diameter	6.25	cm
Length	20	cm
Area	1.4	m^2
V_{Shell}	400	mL
V_{Lumen}	150	mL
Fibre inner diameter	240	μm
Fibre outer diameter	300	μm
Number of fibres	9 950	
Flow	52.5	L/h

PX mass transfer experiments were performed using a bench-scale setup as shown in Figure 3-2. The synthetic feed (or industrial PLS where applicable) and solvent were circulated over a 1.4 m^2 3M™ Liqui-Cel™ EXF-2.5x8 module in two separate circuits. The feed and solvent volumes for respective experiments were chosen so that it took between 1 and 2 hours to extract 90 % of the metal. This implies that the transfer per pass was negligible, which is required for the mass transfer equation for batch processes (discussed in Section 2.5). Samples of the aqueous phase were taken at regular intervals and analysed using ICP-OES (Agilent 5110). In addition, the pressure drops for both circuits that were used in the hydrodynamic design of the plant were recorded, while the pH of the aqueous phase was measured (Metrohm 744, 6.0258.010 electrode). By repeating specific experimental data points, an experimental error for the PX data was found to be < 6.4 %. The error was calculated by determining the standard deviation and subsequently converting this to a percentage value relative to the average value of the repeated data points.

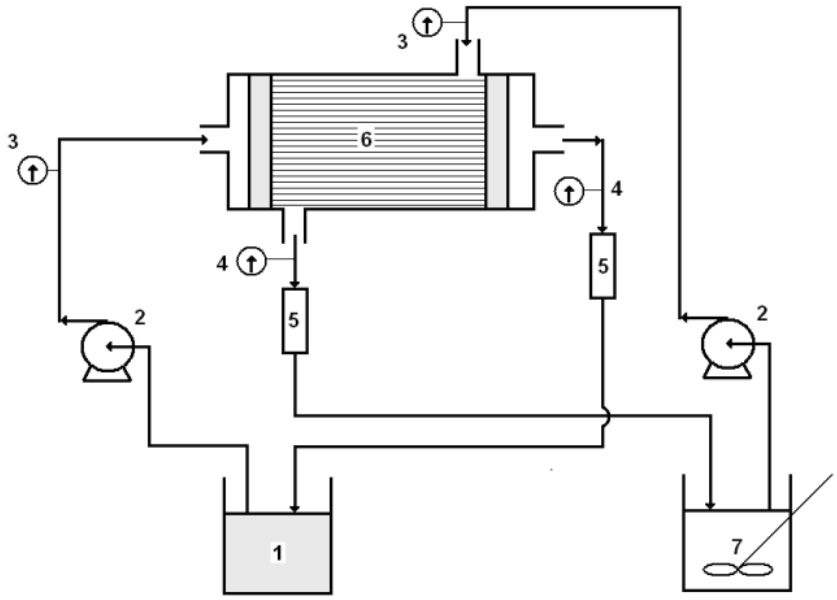

Figure 3-2. Laboratory-scale 1.4 m^2 PX setup for mass transfer measurements, with 1) the organic reservoir, 2) gear pumps, 3) inlet pressure gauge, 4) outlet pressure gauge, 5) flow meters, 6) hollow fibre membrane contactor and 7) the aqueous reservoir. Used with permission of the author.[5]

3.3.1) Extraction

3.3.1.1) Shell vs lumen

As mentioned previously, the membrane contactor consists of two sides, i.e. the shell and the lumen side. The shell side refers to the area surrounding the membrane hollow fibres whilst the lumen refers to the area inside the fibres. To determine the optimal solvent feed side, the solvent was fed through the shell side of the module and then compared to a run where the solvent was fed through the lumen side. During both experiments, the flow and volume of both phases were 875 mL/min and 700 mL, respectively. The synthetic feed consisted of 1.065 $\pm$ 0.005 g/L Co and 11.017 $\pm$ 0.035 g/L Ni. In both cases, the solvent consisted of 9 wt% C272 (50 % pre-neutralised using ammonia solution) and 5 %(v/v) 1-octanol diluted in Shellsol 2325.

3.3.1.2) Distribution coefficient enhancement effect

To assess the mass transfer enhancement via the distribution coefficient, the mass transfer kinetics of a synthetic feed solution consisting of 1.03 g/L Co (and 10.80 g/L Ni) were compared to that of a feed solution consisting of 4.41 g/L Co (and 11.13 g/L Ni). The appropriate amount of sulphate salts were dissolved in deionized water and the pH adjusted to values between 5.0 and 5.5. The solvent consisted of 22 wt% C272 (50 % pre-neutralized using ammonia solution) and 5 %(v/v) 1-octanol diluted in Shellsol 2325. In both cases the flow rate and phase volumes were 875 mL/min and 700 mL, respectively.

3.3.1.3) Extractant concentration

To determine the effect of C272 concentration on the PX mass transfer kinetics of Co and Ni, the extraction behaviour of a 9 wt% C272 solvent was compared to that of a 22 wt% solvent. In both cases the C272 was pre-neutralised (to the extent of 50 %) and 5 %(v/v) 1-octanol was used as the phase modifier in the solvent. Synthetic feed solutions that contained 1.04 ± 0.01 g/L Co and 10.93 ± 0.12 g/L Ni were prepared by dissolving the appropriate amount of hydrated sulfate salts in deionised water. The flow rate and volume of both the feed and solvent in the PX setup was 875 mL/min and 700 mL, respectively. The pH values of the two feed solutions were adjusted to values between 5.0 and 5.5 prior to extraction.

3.3.1.4) Impurities

The industrial PLS supplied by Minemet PTY(LTD) contained trace amounts of impurities after having been processed at the Minemet plant (process discussed in Section 1.1). To assess the effect that the impurities had on the mass transfer kinetics of Co, the extraction behaviour of the industrial solution (after filtration) was compared to the behaviour of a similar synthetic solution. The industrial solution (obtained from Minemet PTY(LTD)) contained 4.70 g/L Co and 10.85 g/L Ni with the following trace impurities: 0.02 g/L Fe, 0.18 g/L Mn and 0.12 g/L Mo. A synthetic feed, containing only 4.41 g/L Co and 10.74 g/L Ni, was prepared by dissolving the appropriate amount of hydrated sulfate salt in deionised water. The pH values of the two feed solutions were adjusted to values between 5.0 and 5.5. During both experiments, a solvent consisting of 22 wt% C272 (50 % pre-neutralised using ammonia solution) and 5 %(v/v) 1-octanol was used. The volume and flow rate of both phases in both experiments were 700 mL and 875 mL/min, respectively.

3.3.2) Scrubbing

From the LLE data, it was evident that a strip liquor consisting of 50 g/L Co at a pH of 5.0 contacted with a loaded solvent at an O/A ratio of 30 was expected to give the best scrubbing results. In PX, this O/A ratio corresponds to a Q_{Org}/Q_{Aq} ratio of 30. As such, a loaded solvent at a flow rate (Q_{Org}) of 875 mL/min was contacted with the strip liquor at a flow rate (Q_{Aq}) of 29 mL/min. A volume of 700 mL of each phase was contacted for 120 min. The loaded solvent was prepared using PX, during which 1 L of the Minemet PLS was contacted with 1L of a 22 wt% C272 solvent according to the aforementioned PX contacting procedure (Section 3.3).

3.3.3) Stripping

According to observations made during the LLE experiments, a strip liquor consisting of 0.1 M H_2SO_4 was expected to deliver the best selectivity during stripping whilst a 0.2 M H_2SO_4 stripping liquor was expected to deliver enhanced mass transfer kinetics. To determine the effect of an increased H_2SO_4

concentration on PX mass transfer kinetics, the strip behaviour of both solutions was compared. Loaded solvents, consisting of 4.44 ± 0.04 g/L Co and 0.71 ± 0.02 g/L Ni, were prepared by PX. During PX, 1 L of Minemet PTY(LTD) PLS was contacted with 1 L 22 wt% C272 solvent for 120 min. The loaded solvents were stripped using 0.1 and 0.2 M H_2SO_4, respectively. During stripping, 700 mL of the loaded solvent was contacted with 700 mL of the strip liquor at 875 mL/min for 240 min.

3.4) References

1. Parhi, P. K.; Panigrahi, S.; Sarangi, K.; Nathsarma, K. C., Separation of cobalt and nickel from ammoniacal sulphate solution using Cyanex 272. *Separation and Purification Technology* **2008,** *59* (3), 310-317.
2. Gabelman, A.; Hwang, S.-T., Hollow fiber membrane contactors. *Journal of Membrane Science* **1999,** *159* (1), 61-106.
3. Schöner, P.; Plucinski, P.; Nitsch, W.; Daiminger, U., Mass transfer in the shell side of cross flow hollow fiber modules. *Chemical Engineering Science* **1998,** *53* (13), 2319-2326.
4. Baudot, A.; Floury, J.; Smorenburg, H. E., Liquid-liquid extraction of aroma compounds with hollow fiber contactor. *AIChE journal* **2001,** *47* (8), 1780-1793.
5. van der Westhuizen, D. J. Pertraction. An innovative technology for the South African Hydrometallurgical industry. PhD thesis, in process.

CHAPTER 4

RESULTS AND DISCUSSIONS

In this study, liquid-liquid extraction (LLE) data were used to identify suitable solutions for extraction, scrubbing and stripping to recover and purify cobalt (Co) from spent hydro treatment catalysts. The solutions identified using LLE data were subsequently used during pertraction (PX) experiments. PX batch runs were performed to optimise Co mass transfer kinetics. The data obtained during LLE and batch PX, in conjunction with the set of models from Table 2-1, were used for the conceptual design of the PX extraction circuit.

4.1) Liquid-liquid extraction

4.1.1) Extraction

As the starting point in the design of a suitable solvent for Co extraction, the following molar ratio was used Co_{Aq}: Cyanex 272 ($C272_{Org}$): NH_4OH_{Org} of 1: 4.8: 2.4. The aforementioned molar ratio resulted in a 3 wt% C272 solvent with a molar addition of 50 % NH_4OH in terms of the $C272_{Org}$ present. This molar ratio was chosen because of the extraction mechanism of pre-neutralised C272, discussed in Section 2.4, and the fact that the supplier of C272 (Cytec) suggests that no more than 55 % of the C272 should be pre-neutralised. A volume of 15 mL of each phase, resulting in an organic to aqueous (O/A) ratio of 1:1, was contacted at 25 ºC for 60 min.

The extraction results obtained with this molar ratio as a function of the feed pH is presented in Figure 4-1. As expected from literature,[1] it is clear that C272 is remarkably selective for Co over Ni with separation factors (SF) as high as 45 obtained at feed pH values > 4. Additionally, it is evident from Figure 4-1 that a maximum of only 53 % Co is extracted at optimal feed pH values when using the above-mentioned molar ratio. This low Co extraction can be attributed to the low loading capacity of the solvent containing only 3 wt% C272, of which 50 % was pre-neutralised using NH_4OH. There are two options available for increasing the loading capacity of the C272 solvent (when maintaining a fixed temperature, O/A ratio and diluent) and these include: (i) increasing the extractant concentration and (ii) increasing the amount of pre-neutralised extractant in the solvent.

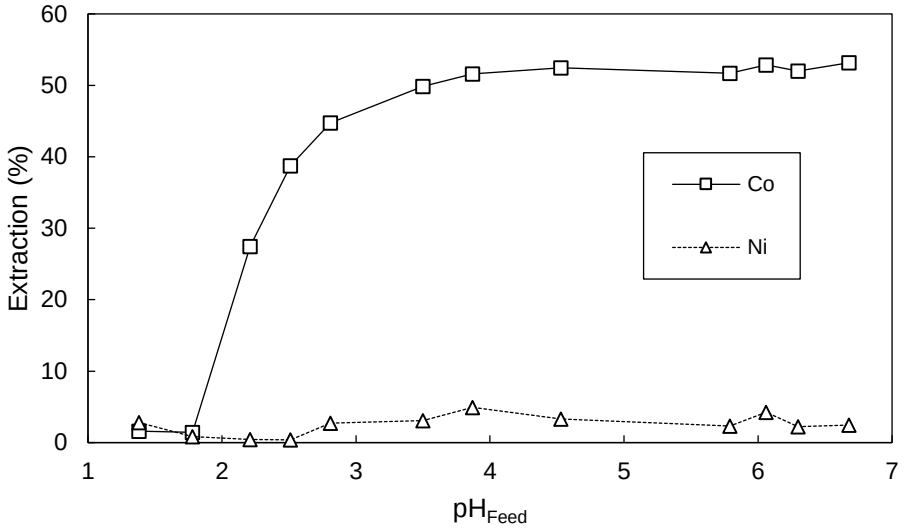

Figure 4-1. Extraction as a function of feed pH. A feed consisting of 1.02 g/L Co and 11.51 g/L Ni was contacted with a 3 wt% Cyanex 272 (50 % pre-neutralised) solvent.

To increase the loading capacity of the solvent, the first step was to investigate the effect of extractant concentration on extraction, whilst keeping the amount of NH_4OH constant at 0.04 M. Feed solutions consisting of 1.04 ± 0.02 g/L Co and 11.62 ± 0.02 g/L Ni were contacted with C272 solvents (3, 9 and 15 wt%) at an O/A ratio of 1:1 at ambient temperature. The result of increasing C272 concentration is given in Figure 4-2. It is evident that increasing the C272 concentration without simultaneously increasing the concentration of the pre-neutralisation agent (NH_4OH) does not significantly increase the loading capacity of the solvent. The increased extractant concentration did, however, reduce the selectivity of the solvent as the Ni extraction slightly increased with increasing C272 concentration. It is therefore evident that the amount of pre-neutralised C272 should also be increased to increase the loading capacity of the solvent. The negative extraction values seen in Figure 4-2 can be attributed to small experimental errors and the values are within the calculated experimental error of 6.2 % as discussed in Section 3.2.

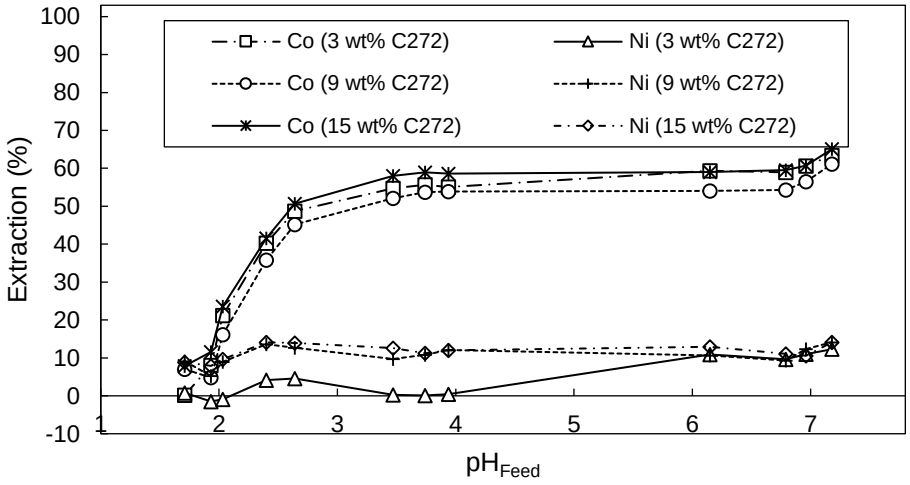

Figure 4-2. Effect of increasing Cyanex 272 concentration on extraction with a constant NH_4OH concentration. Feeds consisting of 1.04 + 0.02 g/L Co (and 11.62 ± 0.02 g/L Ni) were used.

During the pre-neutralisation of C272 (using an ammonia solution), the ionisable proton on the extractant is exchanged with an NH_4^+ ion according to Eq. 8.[2]

$$NH_4OH_{Aq} + HR_{Org} \rightleftharpoons NH_4R_{Org} + H_2O_{Aq} \quad (7)$$

Figure 4-3 shows the effect of pre-neutralisation on the loading capacity of the solvent when determining the extraction as a function of the feed pH using two NH_4OH concentrations (0.04 and 0.18 M) to pre-neutralise the solvent. In this case the feed solutions contained 1.06 ± 0.01 g/L Co and 11.11 ± 0.14 g/L Ni that were contacted with a 15 wt% C272 solvent in an O/A ratio of 1:1. From Figure 4-3, it is evident that increasing the amount of pre-neutralised extractant from 10 % to 50 % increased the loading capacity of the solvent considerably. This finding coincides with results obtained by Könighofer, et al. [1], who showed that 99 % Co extraction could be obtained from a 1 g/L feed solution when using pre-neutralization. Using a 15 wt% solvent that contained 10 % pre-neutralised extractant, a maximum of 53 % Co was extracted from the 1 g/L Co feed solution. When the pre-neutralisation was increased to 50 %, the maximum Co extraction increased to 98 % above feed pH values of 2. The increased extraction can be explained when one compares the extraction mechanism for C272 (Eq. 9) to the extraction mechanism for pre-neutralised C272 (Eq. 10).

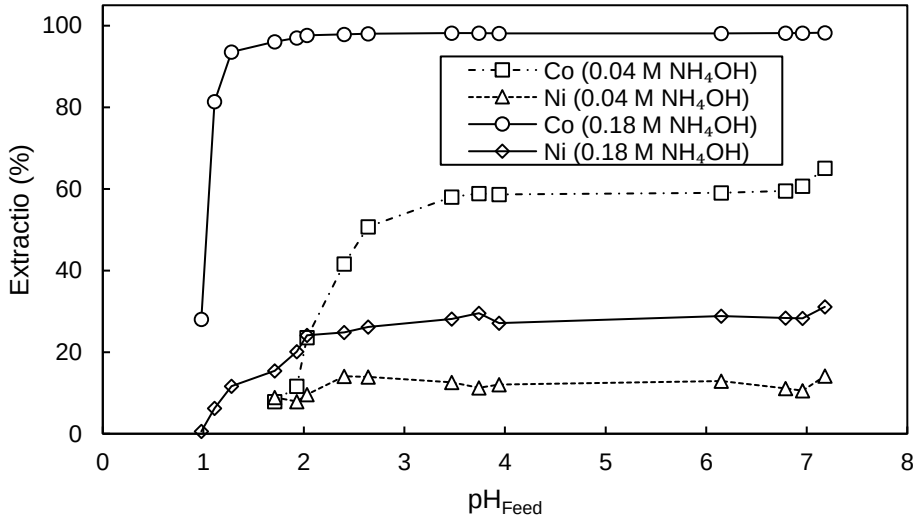

Figure 4-3. Effect of increasing pre-neutralized extractant. 15 wt% Cyanex 272 solvents were contacted with feeds consisting of 1.06 ± 0.01 g/L Co and 11.11 ± 0.14 g/L Ni.

$$Co^{2+}_{Aq} + 2(HR)_{Org} \rightleftharpoons CoR_{2,Org} + 2H^{+} \quad (8)$$

$$Co^{2+}_{Aq} + 2NH_4R_{Org} \rightleftharpoons CoR_{2,Org} + 2NH_4^{+} \quad (9)$$

From Eq. 9 it is evident that extraction with C272 that has not been pre-neutralised, involves proton generation, implying that the extraction requires the continuous addition of a base to shift the equilibrium of the reaction to the right to maintain sufficient extraction. On the contrary, the reaction mechanism of the pre-neutralised C272 does not involve proton generation (Eq. 10) and therefore continuous pH control is not required. This was confirmed by determining the equilibrium pH of Co when extracting with 10 % and 50 % pre-neutralised C272 (Figure 4-4). While maximum Co extraction was expected at an equilibrium pH ≥ 5.0,[1, 3] the equilibrium pH attained with the 10 % pre-neutralised C272, without continuous pH control, was 4.48 ± 0.07, resulting in low Co extraction. These findings coincide with results obtained by Könighofer, et al. [1] who showed that optimal Co extraction (and separation from Ni) is obtained at pH values between 5.0 and 5.5.

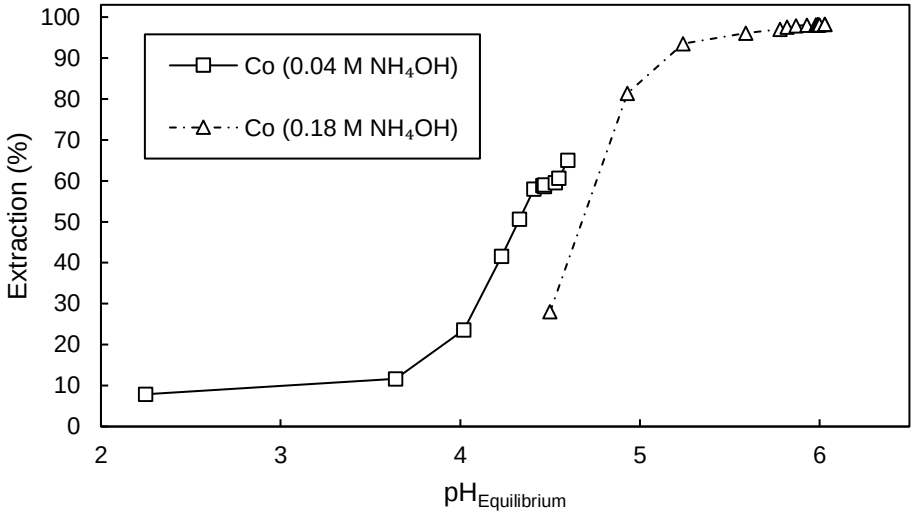

Figure 4-4. pH dependence of Co extraction (with 10 and 50 % pre-neutralised Cyanex 272).

From Figure 4-3, it is evident that increasing the amount of pre-neutralised extractant did not only increase the Co extraction, but also decreased the selectivity of the solvent. This can be attributed to the fact that Ni extraction also increased with increasing pre-neutralisation. Könighofer, et al. [1] found that Ni extraction starts at equilibrium pH values of ≥ 5.5. As shown in Figure 4-4, the equilibrium pH of 50 % pre-neutralised C272 exceeds 5.5, resulting in increased Ni extraction. For optimal separation in addition to maximum extraction, optimisation of the amount of NH_4OH is therefore also required.

The selectivity dependence on the NH_4OH concentration (in the solvent) when extracting with a 9 wt% C272 solvent is presented in Figure 4-5. It is evident that the Co extraction reached a maximum when 50 % of the C272 had been pre-neutralised (0.21 M C272 and 0.10 M NH_4OH). Below 50% the tendency shown previously was confirmed, i.e. a decrease of the % extraction albeit with high selectivity. Above 50 %, an increase in the C272 pre-neutralisation resulted in a linear increase in the Ni extraction, whereas the Co extraction remained at a maximum, resulting in a decrease in selectivity. Additionally, it is not recommended to neutralise more than 55 % of the extractant as, according to the supplier of C272,[3] this may lead to third phase formation.

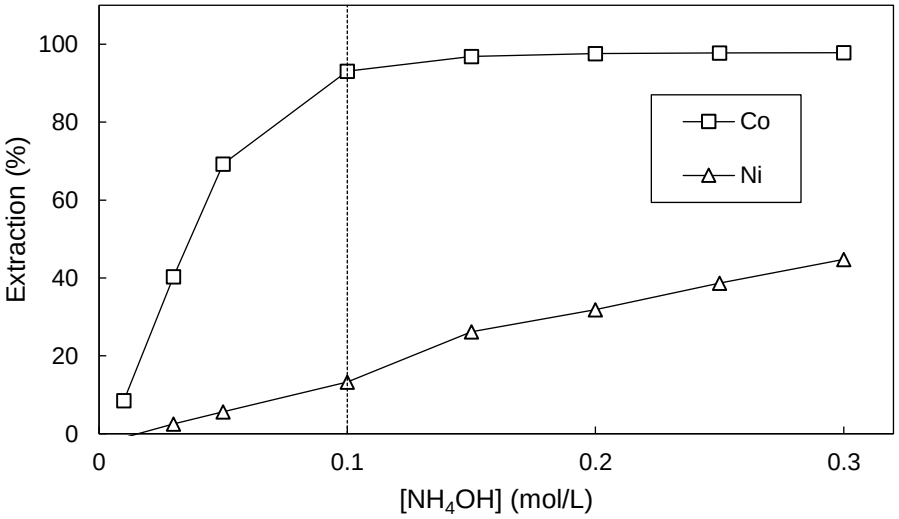

Figure 4-5. Co/Ni extraction as a function of NH_4OH concentration in a 9 wt% Cyanex 272 solvent, with the dotted line indicating the moment when 50 % of the solvent is pre-neutralised.

From these results, the optimal solvent would therefore consist of a 50 % pre-neutralised 22 wt% C272 solution, while optimal Co extraction and separation would be obtained when working at equilibrium pH values ranging between 5.0 and 5.5.

In view of the high concentration of Co in the PLS supplied by Minemet PTY(LTD) (see Table 3-2), a solvent having a sufficient loading capacity would be required to efficiently extract the Co from the supplied PLS. As a result, the Co loading capacity of various concentrations of the C272 solvent (50 % pre-neutralised) was investigated, of which the results are given in Figure 4-6. As expected, the equilibrium concentration in the solvent increased with increasing C272 concentration. From these results, the distribution coefficients for the feed (D_F) and raffinate (D_R), solvent-to-feed ratios and the calculated solvent viscosities are given in Table 4-1. Accordingly, the distribution coefficients at the feed side were typically one or two orders of magnitude lower than those on the raffinate side. For a fair comparison of the solvents, the geometric mean of the distribution coefficients, $D_{gm} = \sqrt{(D_F D_R)}$ was used, as is common practice in distillation.[4] As seen in Table 4-1, the D_{gm} values increased from 0.642 in the 9 wt % solvent, to 32.3 in the 22 wt% solvent, implying that the optimal distribution in pertraction (PX) would be expected with a solvent consisting of 22 wt % C272. Swain, et al. [5] also found that the distribution increases with increasing C272 concentration. The minimum O/A ratio, for the various solvents, were calculated using the solvent to feed ratio equation (Table 2-1). The results are given in Table 4-1, as expected the minimum O/A ratio decreases as the extractant concentration in the solvent increases. Solvent viscosities, μ_0, were calculated using the Kendall-Monroe equation as discussed in Section 2.5.[6] The viscosity of the solvent also increased from 3.03 (at 9 wt% C272) to 5.46 mPa.s at 22 wt% C272. Soldenhoff, et al. [7] found that an increased viscosity can result in a decrease in diffusivity during PX. Based on the higher distribution, the 22 wt% C272 (50 %

neutralized using NH_4OH) was expected to have the best PX characteristics. The increased viscosity which could lead to a decrease in diffusivity should however, be kept in mind.

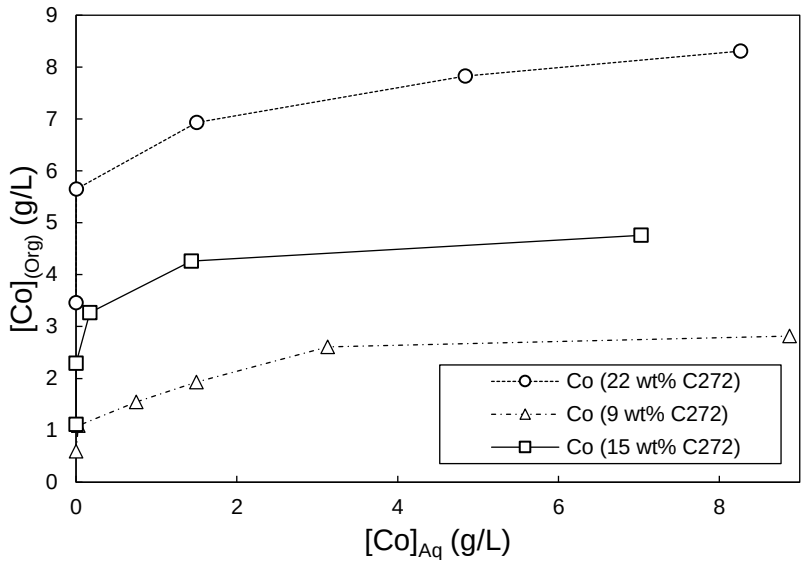

Figure 4-6. Distribution isotherms for Co extraction using 9, 15 and 22 wt% Cyanex 272 solvents, respectively.

Table 4-1. Distribution coefficients for feed, raffinate, solvent-to-feed ratio and calculated viscosities of various solvent concentrations.

[C272] (wt%)	D_F	D_R	D_{gm}	O/A ratio	μ_0 (mPa.s)
9	0.642	107	8.3	1.87	3.03
15	1.122	315	18.8	1.07	4.18
22	1.848	565	32.3	0.65	5.46

4.1.2) Scrubbing

Industrially the most convenient scrubbing solution is the advance Co electrolyte, which consists of $\geq$ 50 g/L Co in H_2SO_4 with pH values between 1.0 and 4.5.[1, 8-10] As the target specification of the final Co product is 50 g/L Co (99.80 %), a similar synthetic solution was chosen as scrubbing liquor. In order to investigate the scrubbing efficiency of the 50 g/L Co electrolyte, a 22 wt% C272 solvent was loaded by contacting the solvent with the PLS supplied by Minemet PTY(LTD) (see Table 3-2). The composition of the loaded solvent obtained (calculated from the mass balance) before scrubbing is given in Table 4-2.

Table 4-2. Composition of loaded solvent used for scrubbing measurements. The loaded solvent contained 22 wt% C272, of which 50 % was pre-neutralised using ammonia solution.

Metal	Concentration in loaded solvent (g/L)
Co	3.48
Ni	0.83
Fe	0.02
Mn	0.17
Mo	0.01

The variables investigated during the scrubbing experiments included the pH (4.0, 4.5 and 5.0) of the scrub liquor and the organic to aqueous (O/A) ratio (30:1, 40:1 and 50:1) between the loaded solvent and the advance electrolyte. In all cases the phases were contacted at 25 ºC for 60 min. The Co- and Ni concentrations in the scrubbed organic for the three O/A ratios, as a function of the scrub liquor pH, are given in Figure 4-7 (A) and (B), respectively. From the figure it is evident that the highest Co concentration in the scrubbed organic was obtained with an O/A ratio of 30:1 using a 50 g/L Co scrub liquor at a pH of 5.0. This was as expected as these conditions relate to the highest amount of the advance electrolyte, relative to the loaded organic, and the optimal pH value for Co extraction derived from results found in the preceding section. Additionally, the O/A ratio of 30:1 gave the lowest Ni concentrations in the scrubbed solvent for all the pH values, compared to that of 40:1 and 50:1. Using the 30:1 O/A, a Co purity of 89.40 % was attained at a pH value of 4.5, and a Co purity of 92.56 % was attained at a pH of 5.0. The slight decrease observed in Ni scrubbing when using the 5.0 pH is thus compensated for by the increased Co extraction.

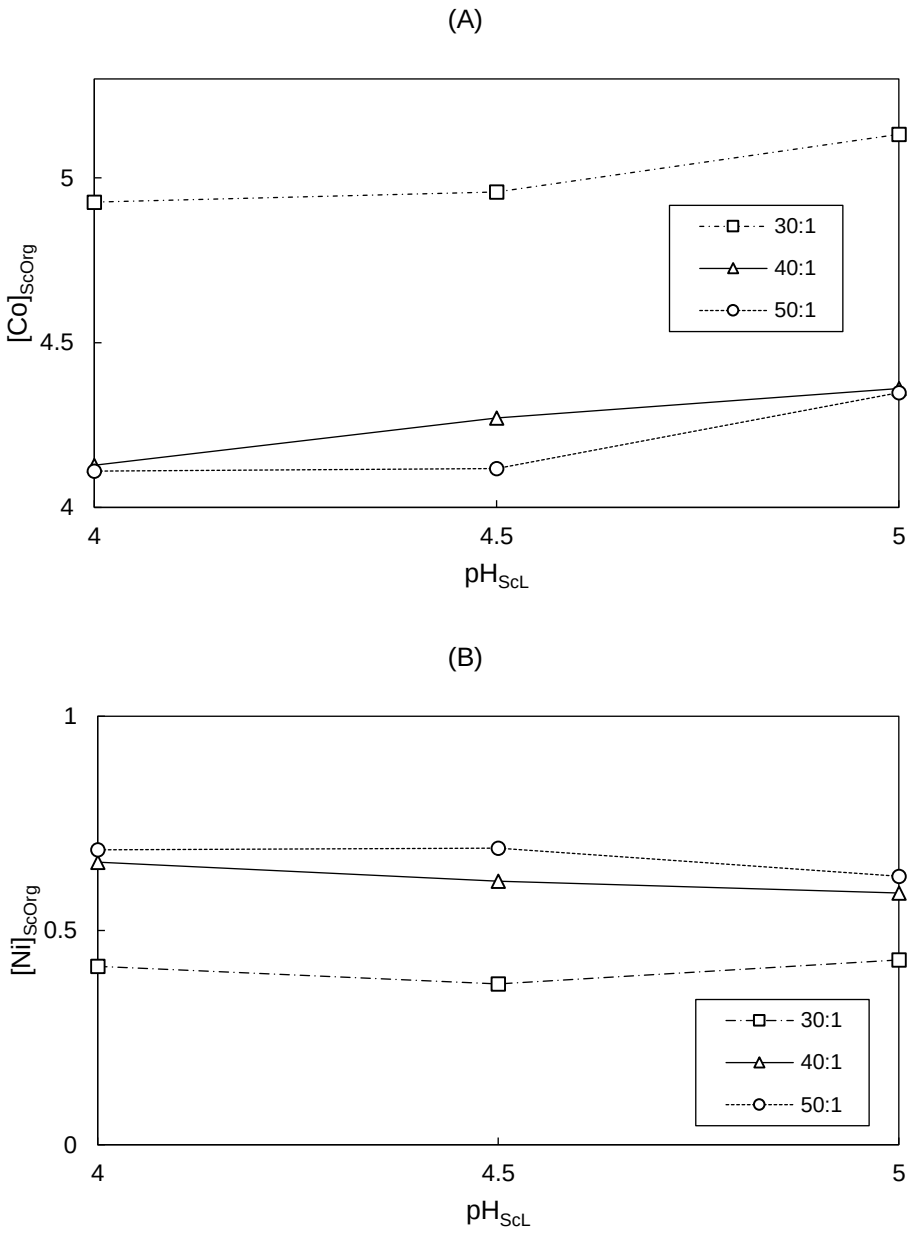

Figure 4-7. Cobalt (A) and nickel (B) concentrations in the scrubbed organic phase as a function of the scrub liquor pH for three O/A ratios. The scrub liquor consisted of 50 g/L Co (98 %).

4.1.3) Stripping

Since electrowinning (EW) of Co is currently done in H_2SO_4 solutions,[11] only H_2SO_4 solutions were used to strip 22 wt% C272 solvents loaded with 1.01 ± 0.003 g/L Co and 1.37 ± 0.085 g/L Ni. The effect of H_2SO_4 concentration on stripping can be seen in Figure 4-8. It is evident that a 0.1 M H_2SO_4 solution sufficiently stripped 100 % of Co from the loaded solvent. At this point, 80 % of the co-loaded Ni was stripped from the loaded solvent. Increasing the H_2SO_4 concentration above 0.1 M increased the amount of Ni stripped from the loaded solvent. Even though the increased acid concentration (> 0.1 M) led to a slightly reduced selectivity of the strip solution, it also slightly increased the rate of the stripping reaction, which was observed by the decrease in time required for the colour of the loaded solvent to change from blue to pale white/yellow and the strip solution from clear to pink.

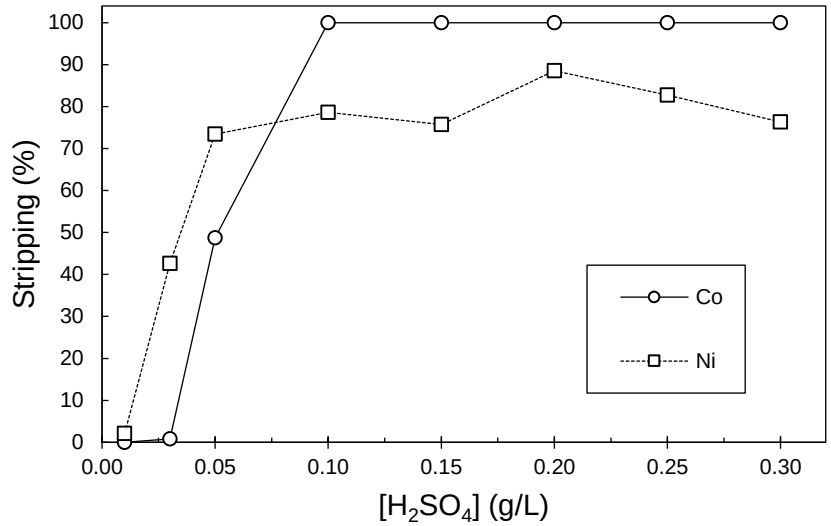

Figure 4-8. Stripping efficiency as a function of H_2SO_4 concentration in the strip liquor.

EW of Co is typically performed from dilute H_2SO_4 solutions between values of 1.0 and 4.5, these values correspond to H_2SO_4 concentrations of 0.1 and 0.2 M, respectively. Outside of these pH values the efficiency of the EW process is reduced and hydrogen incorporation (which causes embrittlement of the metal) is increased.[11] Accordingly, the loading isotherms of both 0.1 M and 0.2 M H_2SO_4 stripping solutions were determined using loaded 22 wt% C272 solvents with varying Co concentrations. The results are given in Figure 4-9. From the figure, the loading capacity of 0.1 M H_2SO_4 could be determined as 5.5 g/L Co. This value coincides with results obtained by Könighofer, et al. [1], who found that the loading capacity of 0.08 M H_2SO_4 as 5.3 g/L Co. It is evident that an increased H_2SO_4 concentration resulted in an increased stripping capacity. The increased loading capacity of the 0.2 M strip liquor was expected when one considers the reaction mechanism shown in Eq. 9, where an increase in acidity will shift the equilibrium of the reaction to the left. The 0.2 M H_2SO_4 stripping also showed faster reactions kinetics compared to that of the 0.1 M solution, which is favourable for the PX refinery as this will lead to a reduced length of the PX stripping column.

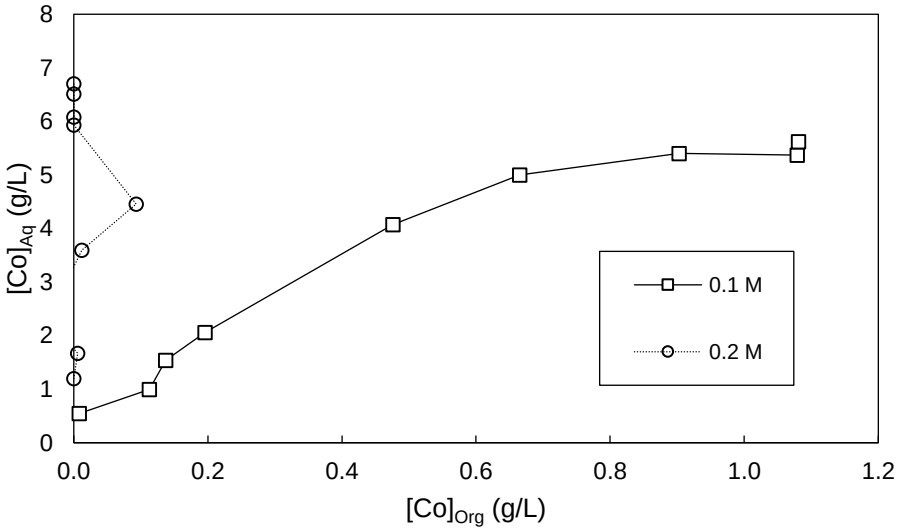

Figure 4-9. Loading capacity of 0.1 and 0.2 M H_2SO_4 strip solutions. Stripping done from loaded 22 wt% Cyanex 272 solvents.

From the LLE data, as previously stated, the most suited solvent in terms of distribution consisted of 22 wt% C272 (50 % pre-neutralised with ammonia solution), which should then also provide the best distribution during the batch PX studies. Additionally, from the equilibrium pH curve shown in Figure 4-4, it is evident that the optimal pH value for extraction is ≥ 5.24, whereas literature suggests that this value is kept under 5.5 to enhance Co/Ni separation[1, 12]. Optimal scrubbing efficiency was obtained with a scrub liquor consisting of 50 g/L Co at a pH value of 5.0. The optimal O/A ratio for scrubbing was found to be 30:1. Finally, it was shown that a 0.1 M H_2SO_4 stripping liquor would deliver the best selectivity, whilst a 0.2 M H_2SO_4 strip liquor would provide preferable mass transfer kinetics.

When processing the Minemet PTY(LTD) PLS (starting at a Co and Ni purity of 29.44 and 68.50 %, respectively) using the aforementioned conditions, it was found that, after extraction with 22 wt% C272 (50 % pre-neutralised), the loaded solvent contained 4.40 g/L Co at a purity of 85.45 % and 0.562 g/L Ni co-extracted. The Ni concentration in the raffinate was found to be 10.71 g/L Ni and the purity increased to 96.69 %, with 0.213 g/L Co remaining in the raffinate. After scrubbing, the Co concentration in the scrubbed solvent increased to 6.0 g/L with a purity of 97 %. Scrubbing removed virtually all the Ni from the scrubbed organic phase, with Mn remaining as the major impurity at 0.17 g/L, contributing 2 % of the scrubbed organic composition. Since Mn does not co-plate during electrowinning of Co metal,[10, 13] it would not affect the purity of the Co product although it is disadvantageous for the anode when using an undivided cell.[10, 13] Ultimately, using a 0.1 M H_2SO_4 strip liquor, a 97 % Co solution could be obtained with 5.69 g/L Co, 0.07 g/L Ni and 0.13 g/L Mn. Alternatively, using a 0.2 M H_2SO_4 strip liquor, a 96 % Co solution containing 6.0 g/L Co, 0.07 g/L Ni and 0.20 g/L Mn was obtained.

4.2) Batch pertraction

4.2.1) Extraction

As it is not straightforward to predict which side (shell or lumen) should be selected as the solvent feed side, two PX experiments were performed where the solvent was first fed through the shell side and then through the lumen side, with all the other experimental conditions kept constant. The extraction as a function of time for these experiments is presented in Figure 4-10. Included are linear regression lines that were applied to the linear regions of the Co curves, i.e. the first 30 min. of both extraction curves. From Figure 4-10, it is clear that supplying the feed to the shell side of the module gave the highest Co extraction rate. These findings coincide with results obtained by Baudot, et al. [14], who found that mass transfer kinetics increased when supplying the feed through the shell side, relative to the lumen, during PX of aromatic compounds.

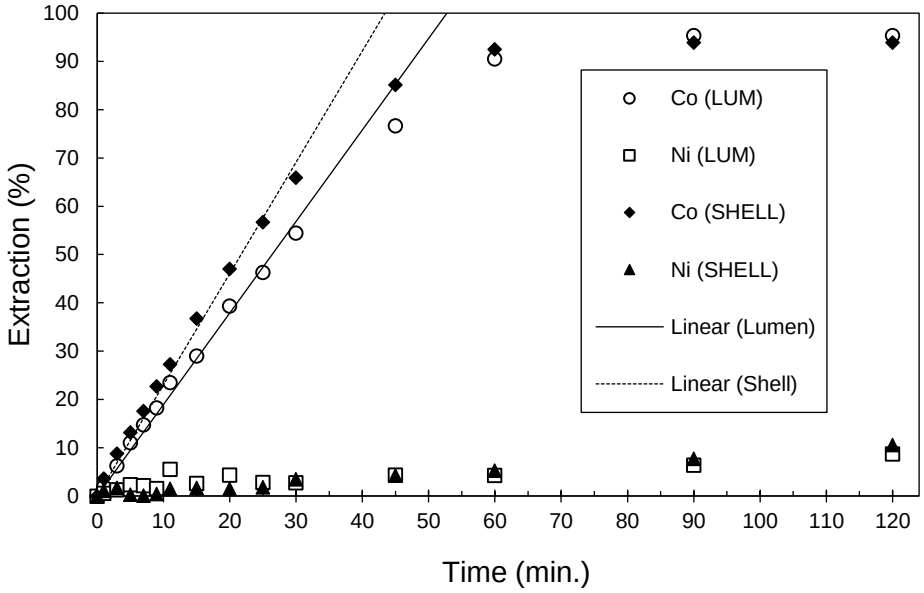

Figure 4-10. Batch pertraction for Co and Ni with the feed flowing through the shell or the lumen side of the module. The feed consisted of 1.06 $\pm$ 0.005 g/L Co and 11.017 $\pm$ 0.035 g/L Ni. In both cases a 9 wt% C272 solvent (50 % pre-neutralised) was used (Experiment 1 and 2).

From the initial slopes of the PX curves (linear regions in Figure 4-10), the overall mass transfer coefficients (k_{ov}) for each experiment were calculated by combining the mass balance and mass transfer equations (given in Table 2-1), yielding Eq. 11.

$$Slope = \frac{1}{x_0}\frac{dy}{dt} = -\frac{1}{x_0}\frac{V_{Aq}}{V_{Org}}\frac{dx}{dt} = \frac{k_{ov}A}{V_{Org}} \quad (10)$$

When calculating the mass transfer coefficients for both curves in Figure 4-10, the mass transfer rate was 20 % higher when the feed was fed through the shell side of the module compared to the

lumen side. This could be ascribed to the fact that the mass transfer resistance is located at the organic interphase (situated at the opposite side of the module where the organic phase is located due to the hydrophilicity of the module). The larger volume of the shell side would, subsequently, lead to an increased extraction rate due to a higher aqueous phase volume. Accordingly, feeding the feed through the shell side of the module would reduce the amount of membrane area required by 20 %. As such, the feed was selected as optimal shell side phase. Additionally, when comparing the mass transfer rate of Co and Ni in both experiments, it was found that the mass transfer rate of Ni was approximately 28 times slower than the mass transfer rate of Co due to the selectivity of the extractant. Once Co has been virtually completely extracted (> 90 % after 60 min.), remaining near constant thereafter, Ni extraction continued from 5 to 11 % for at least another hour as shown in Figure 4-10. Therefore, the extraction and purification in a continuous PX column would most likely also be driven by both equilibrium and kinetics. The mass transfer analysis of these experiments can be seen in Table 4-3, together with the mass transfer analysis of results presented hereafter. This data will be discussed after presenting the pertaining experiments (1-5).

Table 4-3. Mass transfer analysis for Co pertraction.

Exp.	Pertraction (Batch runs)					Baudot, et al. [14]	Minemet PTY(LTD) plant (Simulated)	
	x_{Co} (g/L)	C272 wt%	$k_{ov,0}$ (m/s)	D_0	k_{MO} (m/s)	k_{Aq} (m/s)	$k_{ov,F}$ (m/s)	$k_{ov,R}$ (m/s)
1	1.07	9	2.08×10^{-7}	1.83	1.14×10^{-7}		6.81×10^{-8}	9.24×10^{-7}
2	1.06	9	1.67×10^{-7}	1.85	9.02×10^{-8}		5.48×10^{-8}	9.06×10^{-7}
3	1.03	22	3.33×10^{-7}	6.48	5.14×10^{-8}	1.00×10^{-6}	8.68×10^{-8}	9.67×10^{-7}
4	4.41	22	8.33×10^{-8}	1.79	4.66×10^{-8}		7.94×10^{-8}	9.63×10^{-7}
5	4.70	22	8.01×10^{-8}	1.85	4.34×10^{-8}		7.43×10^{-8}	9.61×10^{-7}

From the loading isotherms in Figure 4-6 and the distribution coefficients presented in Table 4-1, the distribution was calculated (D_0 = 1.77) at the start of a PX experiment with a 9 wt% C272 solvent and a 1 g/L Co feed. After 70 % extraction of the Co, the Co concentration had decreased to 0.3 g/L Co and the distribution coefficient had increased to D_{70} = 2.98. From the resistance-in-series model, given in Eq. 12 it was predicted that the overall mass transfer coefficient increased via the Dk_{MO} term.

$$\frac{1}{k_{ov}} = \frac{1}{k_{aq}} + \frac{1}{Dk_{Mo}} \tag{11}$$

This so-called “distribution coefficient enhancement effect” or D-enhancement effect for overall mass transfer coefficient plays an important part in the design of a continuous PX column. Unfortunately, this D-enhancement cannot be quantified using the results presented in Figure 4-10.

To assess the mass transfer enhancement effect by distribution coefficient, the Co feed concentration was changed from 1 g/L Co to 4 g/L Co. According to the mass transfer model, this should result in a decrease in the overall mass transfer coefficient via the Dk_{MO} term because the distribution coefficient for the 22 wt% C272 solvent decreased from 6.48 at 1g/L Co to 1.79 at 4 g/L Co. The results of these two experiments are given in Figure 4-11. From the results, the D-enhancement effect is clearly visible. The increased distribution, from 1.79 at 4 g /L Co to 6.48 at 1 g/L Co, resulted in a 75 % increase in the overall mass transfer coefficient, as shown by the mass transfer analysis given in Table 4-3. The D-enhancement effect is therefore not only valid for PX of aromatic compounds, as shown by Baudot, et al. [14], but also for metal PX. Additionally, a higher Co concentration led to lower Ni extraction due to the fact that less C272 was available for Ni extraction.

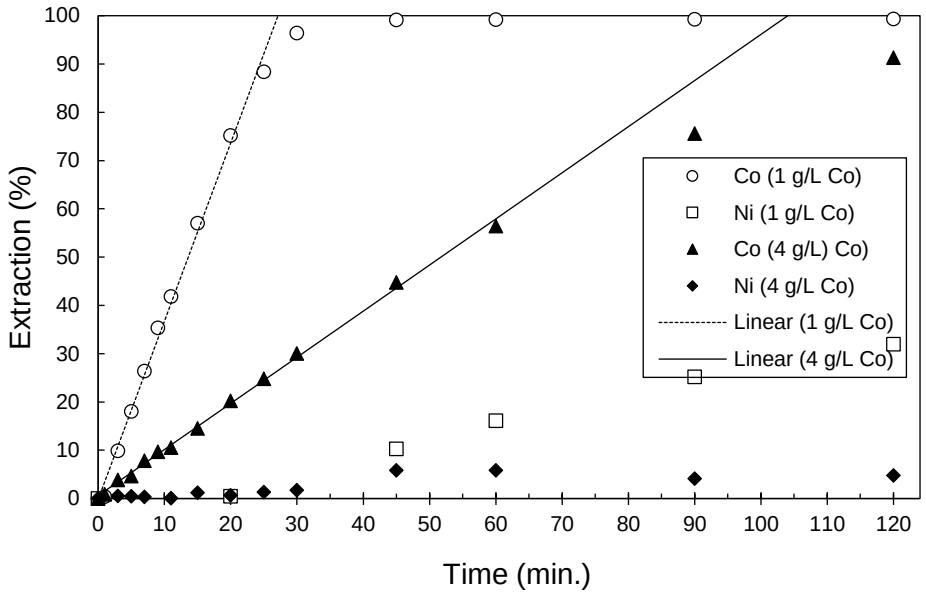

Figure 4-11. D-enhancement of mass transfer at lower Co concentrations. Feed solutions of 1 and 4 g/L Co containing 10 g/L Ni were used (Experiments 3 and 4).

To determine the effect of the C272 concentration on PX extraction, two previously conducted and discussed batch runs (Exp. 2 & 3) were compared in Figure 4-12 using 9 and 22 wt% C272 solvents, respectively, for a 1 g/L Co containing 10 g/L Ni feed. As was expected, the Co mass transfer rate increased considerably with the higher C272 concentration in the solvent. As shown in Table 4-3, the overall mass transfer coefficient was calculated as 1.67×10^{-7} m/s at 9 wt% C272. This value increased by 50 % when using the 22 wt% solvent (3.33×10^{-7} m/s). The counter-effect of an increased viscosity at the higher C272 concentration, which results in a decrease in diffusivity, was

evidently less pronounced. From Figure 4-11, Figure 4-12 and, to a lesser extent Figure 4-10, it can also be seen that Ni extraction only started once Co extraction had been virtually completed. This could open an operating window to increase the Co purity of the extract in a continuous PX column and thus decrease the Ni scrubbing effort required to purify the extract.

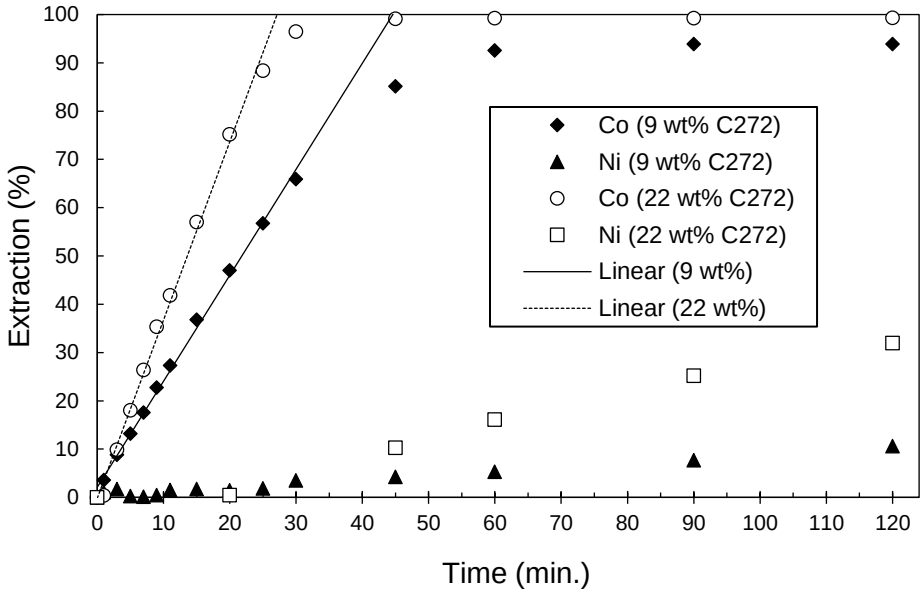

Figure 4-12. Effect of Cyanex 272 concentration on pertraction mass transfer rate. Extractions performed from feed solutions containing 1.04 ± 0.01 g/L Co (Experiments 2 and 3).

Figure 4-13 shows the PX extraction curves from a typical Minemet PTY(LTD) PLS (composition given in Table 3-2) and a similar synthetic solution (4.410 g/L Co, 10.739 g/L Ni) using a 22 wt% C272 solvent. The initial slopes of both extraction curves were practically identical and, subsequently, the overall mass transfer coefficients were within 4 % of one another (see Table 4-3). Könighofer, et al. [1] found that both Mn and Fe are preferentially extracted over Co. As such, the slight delay in Co extraction of the industrial solution can be attributed to the small amounts of Fe and Mn present in the sample. Additionally, virtually no Ni extraction was observed with the Minemet PTY(LTD) PLS. The absence of Ni extraction could also be a consequence of impurity (Fe, Mn) co-extraction suppressing Ni extraction, considering the fact that these metals are preferentially extracted.[1]

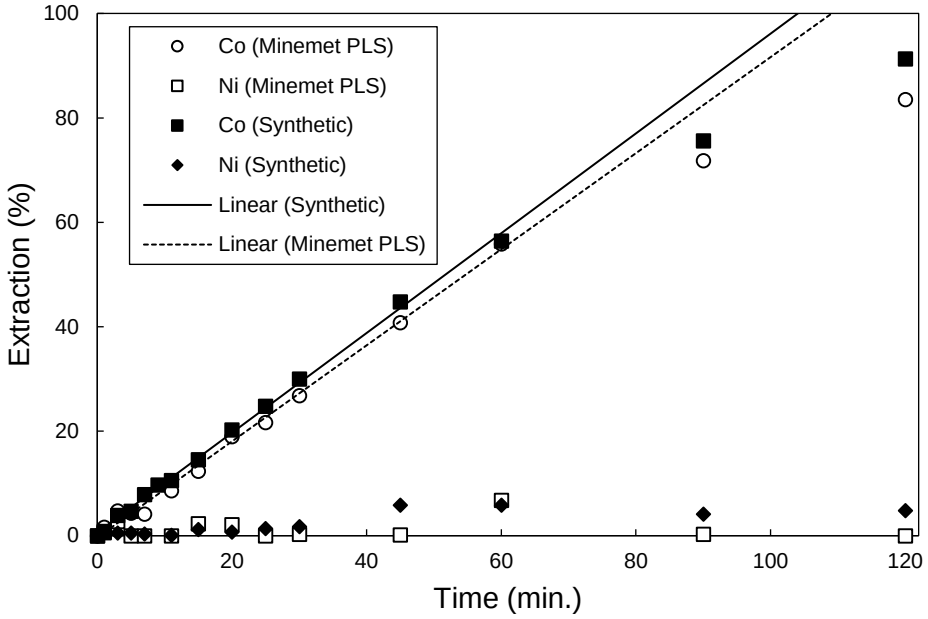

Figure 4-13. Batch pertraction of Minemet PLS and a similar synthetic feed (Experiments 4 and 5).

Baudot, et al. [14] have analysed mass transfer at the aqueous shell side via a Sherwood relation in the same module as used in this study. The results were confirmed experimentally. Independent of the compound extracted, the mass transfer coefficient at the aqueous shell side (k_{Aq}) for a flow rate of 875 ml/min was 1 x 10^{-6} m/s. Additionally, as this is at almost an order of magnitude higher than the initial Co/Ni data measured in this study, it may be assumed that D_{kMo} is the rate limiting term step and thus the k_{Mo} can be calculated from $k_{ov,0}$. The k_{MO} values (given in Table 4-3) were subsequently calculated as $k_{ov,0}/D_0$. At 9 wt% C272, the k_{MO} was 1.0 ± 0.1 x 10^{-7} m/s while being 4.7 ± 0.4 x 10^{-8} m/s at 22 wt% C272. The ~50 % decrease in k_{MO} can be attributed to the high viscosity of the 22 wt% solvent (5.46 mPa.s – see Table 4-1).

Included in Table 4-3 are the simulated overall mass transfer coefficients at the feed ($k_{ov,F}$) and raffinate ($k_{ov,R}$) sides of the Minemet PTY(LTD) PX plant for Experiments 1-5. These values were calculated using the resistance-in-series model, with k_{Aq} = 1 x 10^{-6} m/s and distribution coefficients for feed and raffinate given in Table 4-1. As shown in Table 4-3, the overall Co mass transfer coefficient for the simulated Minemet PTY(LTD) plant increased more than a hundredfold when moving from the feed ($k_{ov,F}$) to the raffinate ($k_{ov,R}$) side, as shown in Table 4-3. The observed increase can be attributed to the D-enhancement effect. The D-enhancement effect was observed in Figure 4-11, which showed that this effect is not only valid for PX of aromatic compounds,[14] but also for metal PX. So, while the driving force for mass transfer decreased from the feed to the raffinate side (decrease in Co concentration), this was compensated for by the increasing overall mass transfer coefficient due to the distribution coefficient. This was further quantified by simulating the PX process as part of the conceptual design process (results presented hereafter).

The mass transfer analysis of the Minemet PTY(LTD) PLS rarely differed from the results obtained for the synthetic solution, implying that synthetic experiments with higher flexibility in feed composition are suitable for analysing the effect of changing distribution coefficients with changing metal concentrations.

To assess the co-extraction of impurities, an experiment was performed during which the extraction of Co, Ni, Fe, Mn and Mo from the Minemet PTY(LTD) PLS was monitored as a function of time. From Table 4-4 it is evident that Mn and Fe were preferentially extracted over Co, whereas Mo was preferentially extracted over Ni. This is as expected when one considers the selectivity of C272, which selectively extracts Mn and Fe over Co.[10, 15] The slight delay in Co extraction, observed in Figure 4-13, is therefore confirmed to be attributed to the co-extraction of impurities from the industrial PLS. The absence in Ni extraction observed with the PX of the Minemet PTY(LTD) sample (Figure 4-13) is, therefore, also attributed to Ni extraction being suppressed by the co-extraction of the trace impurities.

Table 4-4. Co-extraction of impurities from Minemet PTY(LTD) PLS. PX performed with 22 wt% Cyanex 272 solvent.

Metal	Concentration in loaded organic (g/L)	Extraction (%)
Co	3.484	75
Ni	0.826	8
Fe	0.015	88
Mn	0.174	96
Mo	0.013	10

pH measurements of the raffinate samples taken during the batch Experiments 1-5 discussed above are presented in Figure 4-14. The first observation is that the pH of the feed changed significantly within the first few minutes of the run. This implies that the initial transfer of protons across the membrane was fast. It is also apparent that the pH levels remained above 4.8, which is sufficient for Co extraction.[1] With the exception of the Minemet PTY(LTD) PLS (Experiment 5), the pH rose during the runs, indicating that the pre-neutralisation of C272 had the desired effect and that the ion exchange reaction, i.e. Co^{2+} for $2NH_4^+$, was not pH-neutral. The pH of the 4 g/L Co (Experiment 4) synthetic feed remained constant for 30-40 minutes, whereas the rise in pH thereafter coincided with Ni breakthrough. To a lesser extent this was also seen in Experiments 1 and 2. From the pH-isotherms,[16] it is known that nickel extraction starts around pH=5.5. The pH of the PLS (Experiment 5) changed the least of all experiments with pH values remaining between 4.8 and 5.2 over the duration of the run. This might have been caused by the buffering effect of the mixed PLS

composition that was absent in the four synthetic feeds. The fact that the pH remained below 5.5 can be a contributing factor to the absence of Ni extraction observed from the PLS.

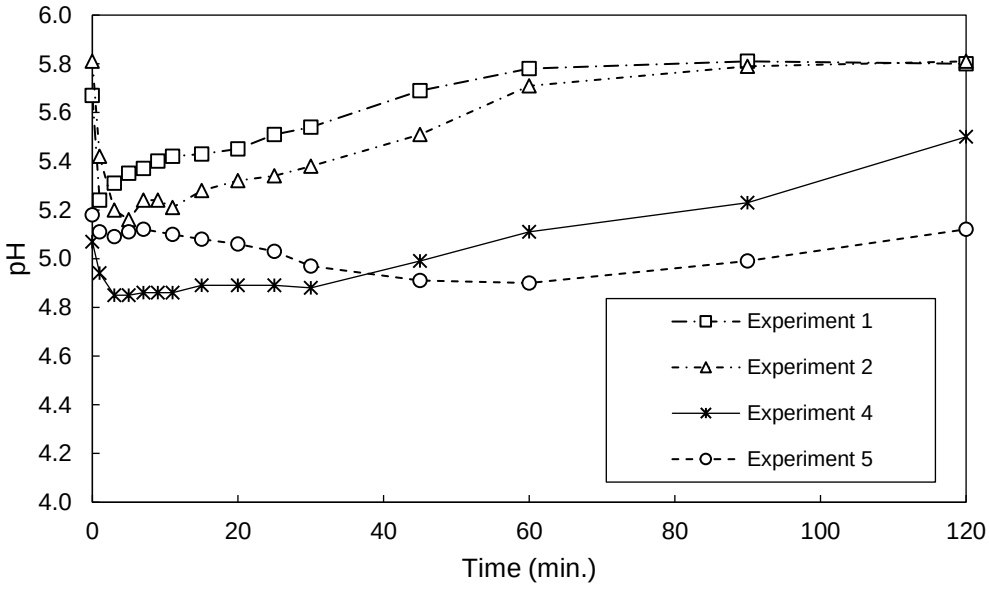

Figure 4-14. pH of aqueous solution as a function of time during the batch pertraction experiments (excluding Experiment 3).

4.2.2) Scrubbing

When using LLE data, the O/A ratio is given by V_{Org}/V_{Aq}, which correlates with the Q_{Org}/Q_{Aq} ratio (organic to aqueous flow rate) in PX. As such, during the PX stripping experiment, the Q_{Org} was 875 ml/min, whereas the Q_{Aq} was 29 ml/min., corresponding to an LLE O/A ratio of 30:1. The composition of the loaded 22 wt% C272 solvent is given in Table 4-5 and a scrubbing liquor consisting of 53.74 g/L Co at a pH of 5 was used. The change in the metal concentration in the organic scrubbing solution over time is given in Figure 4-15. Co extraction from the scrubbing liquor reached equilibrium within 30 min. due to the high driving force as a consequence of the high Co concentration in the scrubbing solution. Ni back-extraction from the loaded organic into the scrub liquor, on the contrary, continued throughout the PX run, resulting in a linear decrease in the Ni concentration throughout the PX run. From the extrapolated linear regression fit of the Ni back-extraction over time, it seems that a PX run of 5 hours would be required to meet the Ni removal target of 0.1 g/L Ni.

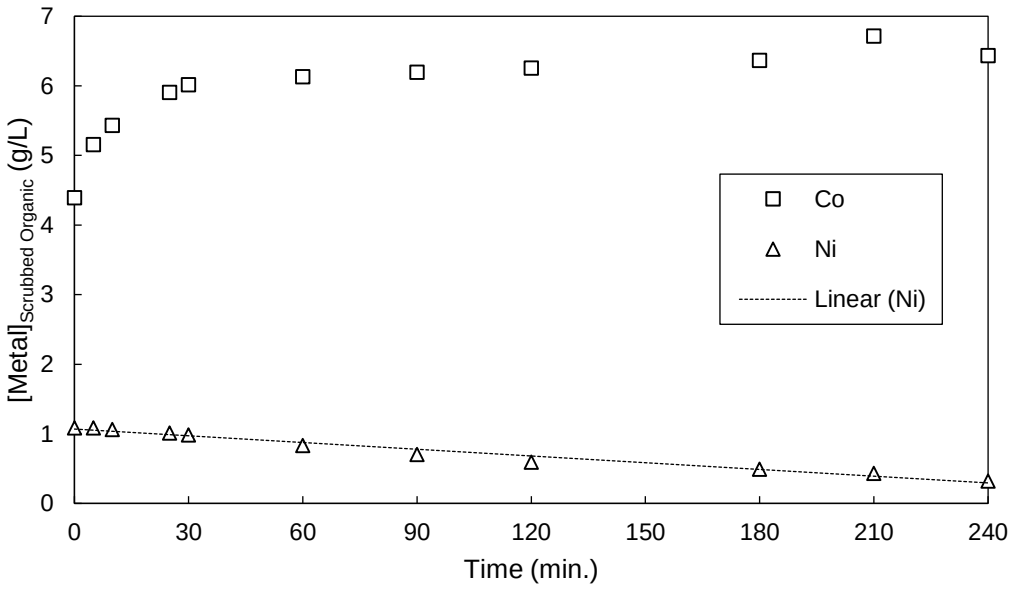

Figure 4-15. PX scrubbing of a loaded solvent containing 4.40 g/L Co, 1.09 g/L Ni and trace amounts of Fe, Mn and Mo. The scrubbing solution consisted of 53.74 g/L Co (≥ 98 %) at a pH of 5.0.

The composition of the loaded organic solvent, prior to and after scrubbing, is given in Table 4-5. Accordingly, the Co purity in the loaded solvent increased from 77.31 %, to 91.10 % after 240 min. of PX scrubbing. Simultaneously, the percentage Ni in the solvent decreased from 19.08 to 4.60 after 240 min of scrubbing. Additionally, the percentage of Mn in the organic phase decreased by 2.15 %, while the amount of Mo increased during scrubbing, which can be attributed to the trace amount of Mo present within the stripping solution prior to contact.

Table 4-5. Composition of organic phase prior to and after PX scrubbing. The organic phase consisted of 22 wt% C272.

Metal	Concentration in loaded solvent (g/L)	Concentration in scrubbed solvent (g/L)
Co	4.40	6.44
Ni	1.09	0.32
Fe	0.01	0.02
Mn	0.17	0.06
Mo	0.02	0.22

4.2.3) Stripping

From the LLE experiments discussed in Section 4.1.3, a 0.1 M H_2SO_4 strip solution was expected to deliver the best selectivity for Co stripping, whilst a 0.2 M H_2SO_4 solution was expected to deliver more favourable mass transfer kinetics. To investigate the effect of an increased H_2SO_4 concentration on the mass transfer kinetics of stripping, the two solutions were compared during a

PX stripping run. 700 mL of the 22 wt% C272 solvent loaded with 4.44 ± 0.04 g/L Co was contacted with 700 mL of the strip liquors for 240 min. The results are given in Figure 4-16. The initial slopes of the stripping curves were practically identical. For the 0.1 M H_2SO_4 stripping solution, the overall mass transfer coefficient was calculated as 5.7 x 10^{-8} m/s, whereas a k_{ov} = 5.1 x 10^{-8} m/s was obtained for the 0.2 M H_2SO_4. The slight initial delay observed when using the 0.2 M H_2SO_4 strip liquor could have been a consequence of the slightly lower Co concentration in the loaded organic (4.48 g/L Co used for the 0.1 M vs. 4.40 g/L Co used for the 0.2 M strip liquor). The fact that both strip liquors showed similar mass transfer kinetics could indicate that the largest mass transfer resistance during PX stripping was located at the membrane (k_{MO}) and was not due to reaction kinetics.[14] In accordance to the LLE data, the 0.1 M strip liquor showed the highest selectivity, whereas the 0.2 M solution had a slightly higher loading capacity after 180 min.

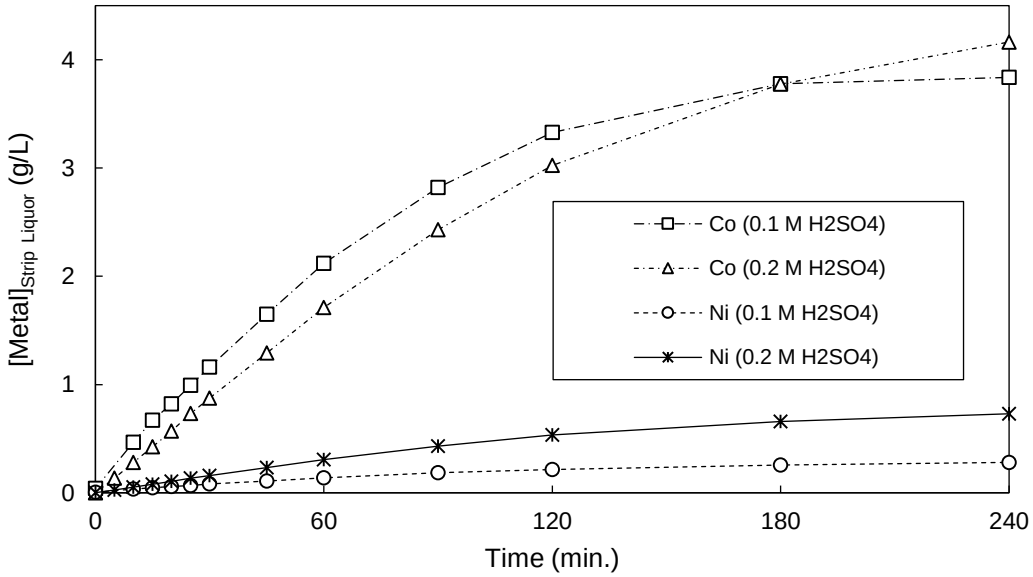

Figure 4-16. Effect of acid concentration in the strip liquor during batch pertraction stripping of 22 wt% Cyanex 272 loaded with 4.44 ± 0.04 g/L Co.

4.3) Conceptual design of the extraction section of a PX refinery

The conceptual design approach in this study had three envisaged outcomes: (i) to determine the concentration profiles over the PX column, (ii) to determine the contact area required and (iii) to obtain the module configuration of the PX column. Since the 22 wt% C272 solvent exhibited the best extraction characteristics according to Section 4.2.1, it was selected as the solvent. The models discussed in Section 2.4 (Table 2-1) in conjunction with the data from the feed composition analysis (Table 3-2), loading isotherms (Table 4-1), mass transfer analyses (Table 4-3), and mass balance (Appendix A, Table A-1) were used to calculate the area required to extract 0.85 kg Co per hour from a feed Co concentration of 4.70 g/L down to a raffinate Co concentration of 0.01 g/L when using an envisaged feed flow rate of 200 L/h (as required by the target specifications).

From the results in Table 4-3, the Minemet PTY(LTD) PLS batch PX run could be modelled and compared to actual experimental data, an example of which is shown in Figure 4-17 for an extraction run. It is evident that the model described the first 30 min. of the PX run correctly. Thereafter, however, the actual Co extraction was faster as the process approached equilibrium. This shortcoming of the model can be attributed to the fact that it does not account for pH changes occurring in the system as the mass transfer model used only takes two physical phenomena into account: i) the driving force, (x-y/D), and ii) the D-enhancement of the overall mass transfer coefficient, Dk_{Mo}. This means that the chemistry in both phases is not included in the variables as this would make the model too complex for process simulation.

This model, including its parameters, was nevertheless used in the conceptual design, knowing that it would probably result in an overdesign of the PX column length. As shown in Figure 4-11 and Figure 4-12, overdesigning the length of the PX column will result in increased Ni extraction and, subsequently, increased scrubbing would be required to purify the extract.

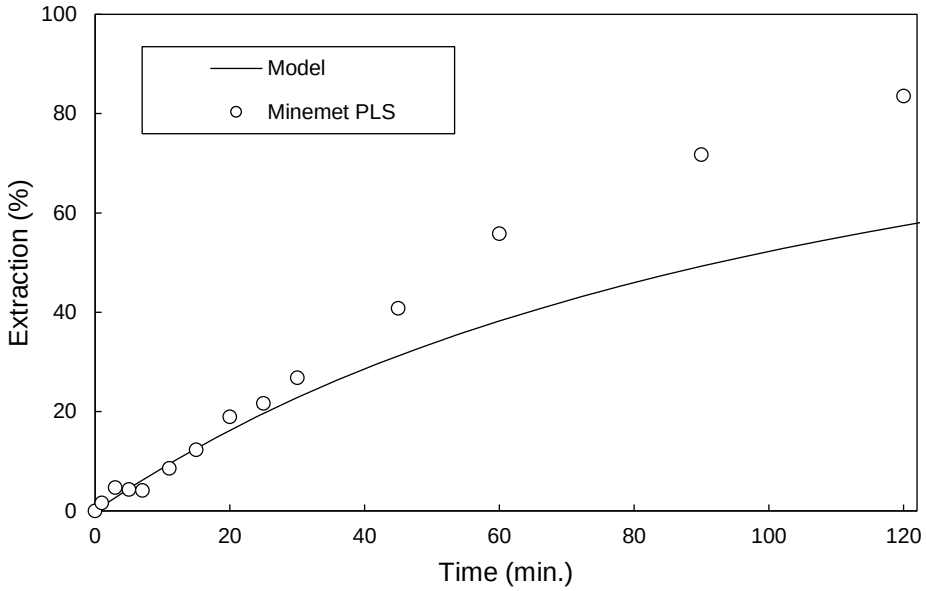

Figure 4-17. Co extraction results of batch pertraction model and Minemet PTY(LTD) PLS pertraction run (Experiment 5).

The PX column profiles obtained for the Co concentration in the aqueous phase and solvent are shown in Figure 4-18. The graph also includes the overall mass transfer coefficient, plotted on the second vertical axis. At the feed side of the column, described by a dimensionless column position, L=0, the overall mass transfer coefficient (k_{ov}) equals 7.43 x 10^{-8} m/s. At approximately L=0.8, there is a fast increase in k_{ov} due to the strong D-enhancement effect below a Co concentration of 2 g/L (x < 2 g/L). For L = 1, the overall mass transfer coefficient (k_{ov}) = 0.96 x 10^{-7} m/s, where it approaches the value of k_{Aq} = 1 x 10^{-6} m/s due to the resistance being dominated by the mass transfer at the

aqueous side. The simulated Co concentration profiles in the aqueous phase, x, and in the organic phase, y, can be understood from this more than tenfold increase of the overall mass transfer coefficient over the length of the column (L=0 to L=1).

The curves in Figure 4-18 were obtained by adjusting the contact area to A = 2125 m^2 in the continuous mass transfer model discussed in Chapter 2.5, which is the area required to ensure that the raffinate meets the given product specification of 0.01 g/L Co, which corresponds to a 99.90 % Ni purity. The area was calculated using the models discussed in Chapter 2.4 (Table 2-1) in conjunction with the data from the feed composition analysis (Table 3-2), loading isotherms (Table 4-1), mass transfer analyses (Table 4-3) and mass balance (Appendix A, Table A-1), as mentioned previously. Also included in the figure is the interphase concentration at the organic side (y_i) and the interphase concentration at the aqueous side (x_i). From the modelled interphase concentrations, it can be seen that the mass transfer resistance is located at the organic interphase, which is situated at the aqueous side of the module due to the hydrophobicity of the module.

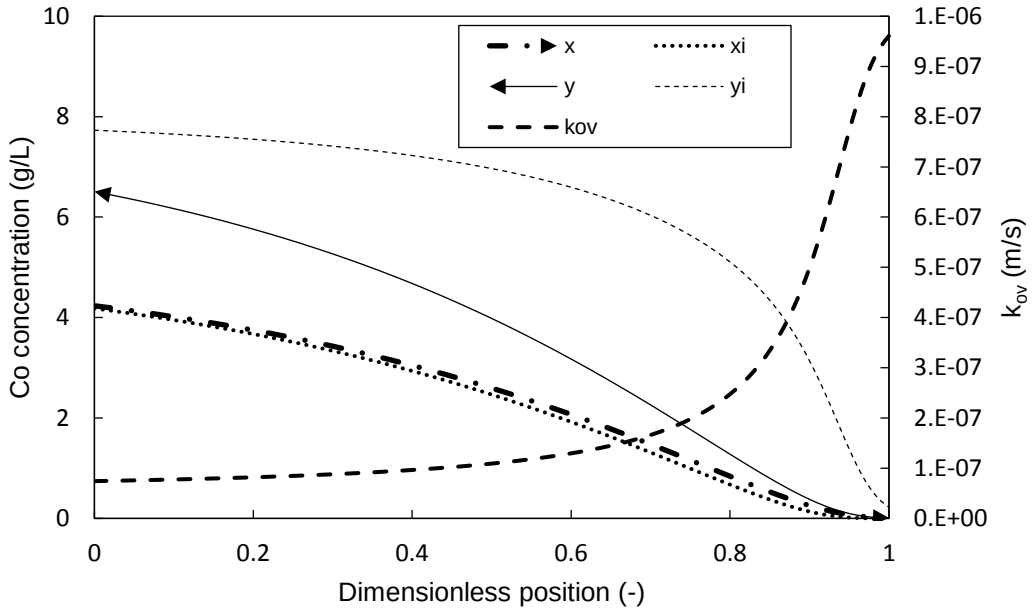

Figure 4-18. Simulated Co concentration profiles in aqueous phase (x) and solvent (y). Arrows indicate flow direction in PX column, where y_i is the Co concentration at the organic interface and x_i the Co concentration at the aqueous interface. x(L=1) = 0.01 g/L Co; y(L=1) = 0 g/L Co; k_{MO} = 4.34 x 10^{-8} m/s; k_{Aq} = 4.34 x 10^{-6} m/s and A = 2125 m^2.

For a contact area of 2125 m^2, 5.7 of the 14x40 XF Liqui-Cel™ modules, in series, would be required, with one of these modules offering a contact area of 373 m^2. Seeing that the number of modules must correspond to an integer, six of these modules were selected for the calculations, which resulted in a raffinate purity of 99.99 %, which is above the 99.9 % Ni target.

Since Ni purification is not a first purification target, a sensitivity analysis was done for a range of Ni purities starting with a feed purity of 67.14 % (Minemet PTY(LTD)) PLS as per calculated mass

balance). The results of the sensitivity analysis are given in Figure 4-19. The dot on the graph indicates the moment when the target raffinate purity is reached (99.9 % Ni). Using a 22 wt% C272 solvent with a single module, the predicted raffinate purity would be 80 % Ni. With three modules in series, this will increase to 92 % Ni. Subsequently, the Ni purity would increase almost linearly up to 99.99 % when six modules were to be used. In order to compare the performance of the 22 wt% C272 solvent to the 9 wt% solvent, the same sensitivity analysis was done for the 9 wt% solvent and the results are also given in Figure 4-19. Accordingly, when using the 9 wt% C272 solvent, the number of modules required to meet the target specification increases to 8. The 9 wt% solvent would therefore require two additional modules in series, which would increase the price of the refinery significantly.

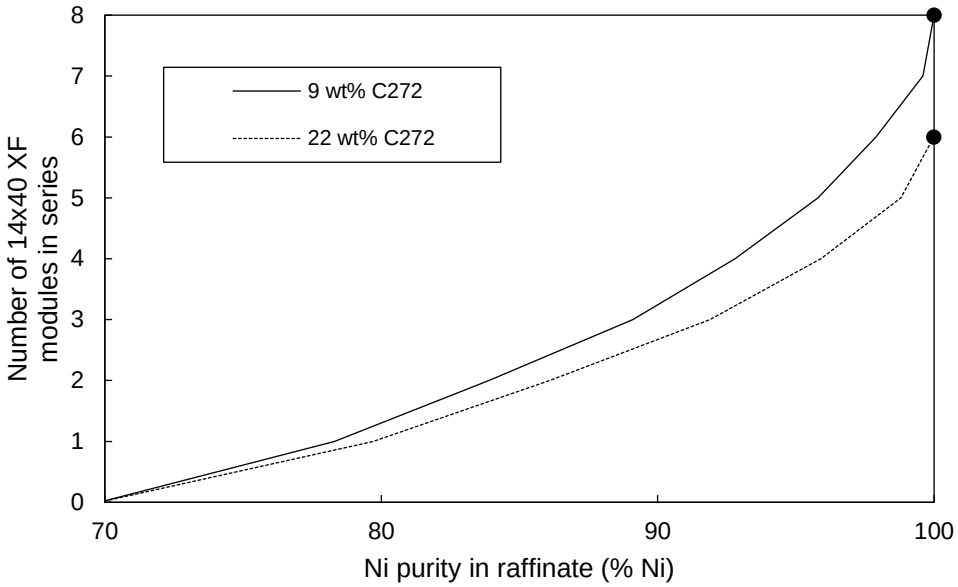

Figure 4-19. Number of 14x40 XF Liqui-Cel™ modules as a function of Ni purity in the raffinate for two C272 solvents, differing in terms extractant concentrations.

4.4) References

1. Könighofer, T.; Archer, S.; Bradford, L., A cobalt solvent extraction investigation in Africa's Copper Belt. *Journal of the Southern African Institute of Mining and Metallurgy* **2009,** *109* (6), 337-342.
2. Hereijgers, J.; Vandermeersch, T.; Van Oeteren, N.; Verelst, H.; Song, H.; Cabooter, D.; Breugelmans, T.; De Malsche, W., Separation of Co(II)/Ni(II) with Cyanex 272 using a flat membrane microcontactor: Extraction kinetics study. *Journal of Membrane Science* **2016,** *499*, 370-378.
3. Szolga, W. In *Flowsheet Developments using Cyanex reagents*, ALTA, Perth, Australia, 20-27 May; Perth, Australia, 2017.
4. Ludwig, E. E., *Applied Process Design for Chemical and Petrochemical Plants*. Elsevier Science: 1997.
5. Swain, B.; Jeong, J.; Lee, J.-c.; Lee, G.-H., Extraction of Co(II) by supported liquid membrane and solvent extraction using Cyanex 272 as an extractant: A comparison study. *Journal of Membrane Science* **2007,** *288* (1), 139-148.
6. Koekemoer, L. R.; Badenhorst, M. J. G.; Everson, R. C., Determination of Viscosity and Density of Di-(2-ethylhexyl) Phosphoric Acid + Aliphatic Kerosene. *Journal of Chemical & Engineering Data* **2005,** *50* (2), 587-590.
7. Soldenhoff, K.; Shamieh, M.; Manis, A., Liquid–liquid extraction of cobalt with hollow fiber contactor. *Journal of Membrane Science* **2005,** *252* (1), 183-194.
8. Feather, A.; Bouwer, W.; Swarts, A.; Nagel, V., Pilot-plant solvent extraction of cobalt and nickel for Avmin's Nkomati project. *JOURNAL-SOUTH AFRICAN INSTITUTE OF MINING AND METALLURGY* **2002,** *102* (8), 457-462.
9. Könighofer, T.; Archer, S. J.; Bradford, L., A cobalt solvent extraction investigation in Africa's Copper Belt. In *Hyrometallurgy Conference 2009*, The Southern African Institute of Minning and Metallurgy: 2009.
10. Swartz, B.; Donegan, S.; Amos, A. In *Processing considerations for cobalt recovery from Congolese copperbelt ores*, Hydrometallurgical Conference, The Southern African Institute of Mining and Metallurgy: 2009; pp 385-400.
11. Lupi, C.; Pilone, D., Electrodeposition of nickel-cobalt alloys: the effect of process parameters on energy consumption. *Minerals Engineering* **2001,** *14* (11), 1403-1410.
12. Swain, B.; Cho, S.-S.; Lee, G. H.; Lee, C. G.; Uhm, S., Extraction/separation of cobalt by solvent extraction: a review. *Applied Chemistry for Engineering* **2015,** *26* (6), 631-639.
13. Mulaudzi, N.; Kotze, M. In *Direct cobalt electrowinning as an alternative to intermediate cobalt mixed hydroxide product*, Base Metals Conference. The Southern African Institute of Mining and Metallurgy. Johannesburg, 2013; pp 209-222.
14. Baudot, A.; Floury, J.; Smorenburg, H. E., Liquid-liquid extraction of aroma compounds with hollow fiber contactor. *AIChE journal* **2001,** *47* (8), 1780-1793.
15. Marcus, Y.; SenGupta, A. K., *Ion Exchange and Solvent Extraction: A Series of Advances*. Taylor & Francis: 2001.
16. Sole, K. C.; Cole, P. M., Purification of nickel by solvent extraction. *Ion exchange and solvent extraction* **2001,** *15*, 143-195.

CHAPTER 5

CONCLUSION, EVALUATION AND RECOMMENDATIONS

5.1) Conclusion

During this study, suitable solutions were identified for extraction, scrubbing and stripping to process pregnant leach solution (PLS), thereby developing a process for the recovery and purification of Co from spent hydro-treatment catalysts. According to the results of Chapter 4, it is clear that pertraction (PX) processing would be suitable for recovering Co from PLS. After optimising process conditions using liquid-liquid extraction (LLE) data on extraction, scrubbing and stripping, mass transfer rates were determined in a batch PX setup and analysed using the resistance-in-series model where three design parameters were identified: D, k_{MO}, and k_{Aq}. A methodology was developed to conceptually design a Co PX extraction column for the purification of Ni as the first section of a Co-Ni PX refinery for processing a PLS of 200 L/h produced from spent hydro-treatment catalysts.

5.1.1) Liquid-liquid extraction

5.1.1.1) Extraction

From LLE results it was evident that, in the absence of continuous pH control, pre-neutralisation of the extractant, Cyanex 272 (C272), was required to increase the loading capacity of the solvent. Additionally, both increasing the C272 concentration and increasing the pre-neutralisation reduced the selectivity of the solvent. It was found that 50 % pre-neutralisation delivered both optimal extraction and selectivity. The distribution isotherms of three C272 solvents were measured using three solvent concentrations, i.e. 9, 15 and 22 wt%. As expected, the equilibrium concentration increased with increasing C272 concentration. The distribution coefficients at the raffinate side were typically one to two orders of magnitude higher than those on the feed side. Through the comparison of the geometric mean of distribution coefficients, D_{gm}, it was found that the 22 wt% C272 had a D_{gm} value that was four times that of the 9 wt% C272 solvent.

From the LLE extraction data, it became evident that a solvent consisting of 22 wt% C272, of which 50 % was pre-neutralised, would have the best PX characteristics both for a simulated as well as a real PLS sample. The 22 wt% C272 solvent extracted 96 % of the Co from the PLS and co-extracted 5 % of the Ni, resulting in a raffinate containing a Ni purity of 97 %.

5.1.1.2) Scrubbing

Since it is common practice to use a small amount of advance electrolyte as scrubbing solution during Co processing, a scrub solution with a Co concentration of 50 g/L was selected as the scrubbing liquor. Design parameters investigated include the O/A ratios and the pH of the scrub liquor. As expected, the lowest O/A ratio (O being the loaded solvent and A the scrub liquor) resulted in the highest Co- and lowest Ni concentrations in the scrubbed organic phase. Subsequently, the highest Co purity was attained when using an O/A ratio of 30:1. Additionally, it was found that the optimal pH to use for the scrub liquor was 5.0. This value coincided with an optimal Co extraction, as was evident from the equilibrium pH isotherms.

The optimal scrubbing liquor was therefore identified as a 50 g/L Co solution at a pH of 5.0 that was contacted with an O/A ratio of 30:1. Through the use of the aforementioned scrubbing solution, the Co purity in the organic phase obtained from the extraction of the Minemet PTY(LTD) PLS could be increased by 12 %. Virtually all the co-extracted Ni could be scrubbed from the organic phase, with Mn remaining as the major impurity.

5.1.1.3) Stripping

The final step in Co metal production is the electrowinning of Co metal from dilute sulfuric acid solutions (pH values between 1.0 and 4.5) as discussed in Chapter 2.6. These pH values correspond to H_2SO_4 concentrations of 0.1 M and 0.2 M. As such, only these two solutions were considered as stripping liquors. It was found that both 0.1 M and 0.2 M H_2SO_4 solutions were suitable to strip Co from the scrubbed organic. The 0.1 M H_2SO_4 solution was found to deliver the highest selectivity whilst the 0.2 M solution gave the most desirable mass transfer kinetics and increased loading capacity.

The 0.1 M H_2SO_4 striping liquor could strip 98 % of Co from the scrubbed organic phase, resulting in a scrub liquor consisting of 5.7 g/L Co at a purity of 97 %. The 0.2 M H_2SO_4 stripping liquor on the other hand stripped 100 % of the Co from the scrubbed organic, resulting in a scrub liquor containing 5.8 g/L Co at a purity of 96 %. In both cases Mn remained as the main impurity, contributing to 2.2 % and 2.9 % of the 0.1 M and 0.2 M strip liquors, respectively.

5.1.2) Batch pertraction

5.1.2.1) Extraction

The first step in the mass transfer optimisation process using PX was to determine the optimal shell side phase. It was found that supplying the feed through the shell side of the module resulted in a

20 % increase in the overall mass transfer coefficient relative to supplying the feed through the lumen side.

According to the resistance-in-series model, the design parameters of importance are k_{Aq}, k_{MO} and D. To assess the effect of the distribution coefficient on the mass transfer kinetics during PX, the PX extraction behaviour of two runs were compared where the distribution was lowered from 6.48 to 1.79. From the results, the mass transfer enhancement via the Dk_{MO} term was clearly visible. Proving that this so-called "distribution enhancement effect" for overall mass transfer coefficient was not only applicable to PX of aromatic compounds, but also for metal PX. It was found that increasing the extractant concentration considerably increased the mass transfer rate; for example a 50 % increase in k_{ov} was observed when increasing the C272 from 9 to 22 wt%.

To assess the influence of the co-extraction of impurities on the overall mass transfer rate, the extraction behaviour of a synthetic solution containing Co and Ni was compared to the extraction behaviour of the Minemet PTY(LTD) PLS, containing Co and Ni with trace amounts of Fe, Mn and Mo. It was found that the presence of impurities had virtually no effect on the mass transfer rate of Co. The co-extraction of impurities did, however, significantly suppress Ni co-extraction. Additionally, a pH buffering effect was observed with the Minemet PTY(LTD) PLS that was absent in the synthetic solutions. It was found that this pH buffering effect contributed to the reduced Ni extraction from the Minemet PTY(LTD) PLS. Furthermore, from pH measurement taken during PX batch runs, it could be shown again during PX that pre-neutralisation had the desired effect by maintaining the pH values of the aqueous samples above 4.8, which is sufficient for Co extraction, making continuous pH control superfluous.

5.1.2.2) Scrubbing

From the LLE results, the optimal scrubbing liquor was identified as a solution consisting of 50 g/L Co at a pH value of 5.0 and optimal organic to aqueous (O/A) ratio was seen to be 30:1. This O/A ratio used in LLE correlates to the Q_{Org}/Q_{Aq} ratio in PX. As such, a Q_{Org}/Q_{Aq} ratio of 30:1 was used during PX scrubbing of the loaded solvent. It was found that Co extraction from the scrubbing liquor quickly reached equilibrium as a result of the high driving force originating from the high Co concentration in the scrub liquor. Ni back-extraction, however, was found to be significantly slower and, as such, the Ni concentration in the scrubbed solvent was found to decrease linearly throughout the duration of the PX batch run.

5.1.2.3) Stripping

From LLE data is was evident that a strip liquor consisting of 0.1 M H_2SO_4 was expected to deliver the highest selectivity, whereas a 0.2 M solution was expected to deliver an increased loading

capacity and improved mass transfer kinetics. During batch PX stripping experiments, however, it was found that both solutions showcased similar mass transfer rates. This showed that the largest mass transfer resistance was due to the transport and diffusion in the module and not due to reaction kinetics. The 0.2 M H_2SO_4 strip liquor did, however, have a slightly higher loading capacity compared to that of the 0.1 M solution, as expected.

5.1.3) Conceptual design of extraction section of pertraction refinery

Through the use of process models (discussed in Section 2.5) together with data from feed composition analyses, loading isotherms, mass transfer kinetics and mass balance, a methodology could successfully be developed for the conceptual design of the extraction section of the PX refinery. The mass transfer model used for the conceptual design of the extraction section described the first 40 min. of the extraction process correctly. Thereafter extraction was, however, faster than predicted as the process approached equilibrium. The inaccuracy of the model can be attributed to the fact that the model does not consider the pH changes that occur during the process, which would, if included, make the model too complex for process simulation. Despite the shortcomings of the model, it was nevertheless used for the conceptual design, knowing that it would result in overdesign of the extraction column which, in turn, would result in the need for increased scrubbing as Ni co-extraction will increase over the length of the column, as seen during batch PX runs.

From the modelling results, when using a 22 wt% C272 solvent, it was found that an area of 2125 m^2 would be required to obtain a Ni purity of 99.9 % in the raffinate. The Liqui-Cel™ 14x40 XF modules deliver a contact area of 373 m^2 each, which thus corresponds to 5.7 of these modules in series. As this number must be an integer, six of these modules were selected which, in turn, results in a raffinate purity of 99.99 %. Alternatively, when using a 9 wt% C272 solvent, the number of Liqui-Cel™ 14x40 XF modules required to reach the Ni target purity would increase to 8.

5.2) Evaluation and recommendations

5.2.1) Liquid-liquid extraction

While the emphasis was not on solvent extraction (SX), it became apparent from the study that Mn cannot be scrubbed from the loaded solvent using the advance electrolyte. Alternative Mn removal options can subsequently be considered. Promising solutions could be the incorporation of a water wash stage or, alternatively, an additional extraction step using a Mn-selective extractant.

Furthermore, it was found that an increased C272 concentration in the solvent resulted in an increased distribution. An increased distribution, in turn, led to an increased extraction rate during

PX. Subsequently, the possibility of using even higher C272 concentrations can be investigated using LLE data.

5.2.2) Pertraction processing of cobalt

During the course of this project a PX process was developed to process a Co/Ni PLS originating from spent hydro-treatment catalysts. The proposed process flowsheet can be summarised as is depicted in Figure 5-1. The PLS (1), containing 4.61 g/L Co and 10.73 g/L Ni (as well as trace amounts of Fe, Mn and Mo), was contacted with a 22 wt% C272 solvent, of which 50 % was pre-neutralised using ammonia solution (10), in order to obtain a raffinate (2) with Ni-purity of 99.99 %. After extraction, the loaded solvent (3) contained 4.0 g/L Co and 1.0 g/L Ni. The co-extracted Ni was then scrubbed from the loaded solvent using a small amount of the advance Co electrolyte (4), which contained ≥ 50 g/L Co at a pH of 5.0. The loaded solvent (3) was contacted with scrubbing liquor (4) at a Q_{Org}/Q_{Aq} ratio of 30:1. Scrubbing ultimately resulted in a scrubbed solvent containing 6.0 g/L Co. After the Ni concentration in the scrubbed organic phase had been reduced to 0.1 g/L Ni, the scrubbed organic (6) was contacted with the strip liquor (7). During this study is was found that a 0.1 M H_2SO_4 solution delivered the best selectivity as a stripping liquor, whereas a 0.2 M solution was found to increase the Co stripping capacity. After the scrubbed solvent was stripped using a dilute H_2SO_4 solution, the stripped organic (9) was pre-neutralised using a base (10), such as ammonia solution or caustic soda, after which the 50 % pre-neutralised solvent (11) was rerouted back to the extraction section. It is assumed that the NH_4 stream leaves as the equivalent amount of $(NH_4)_2SO_4$.

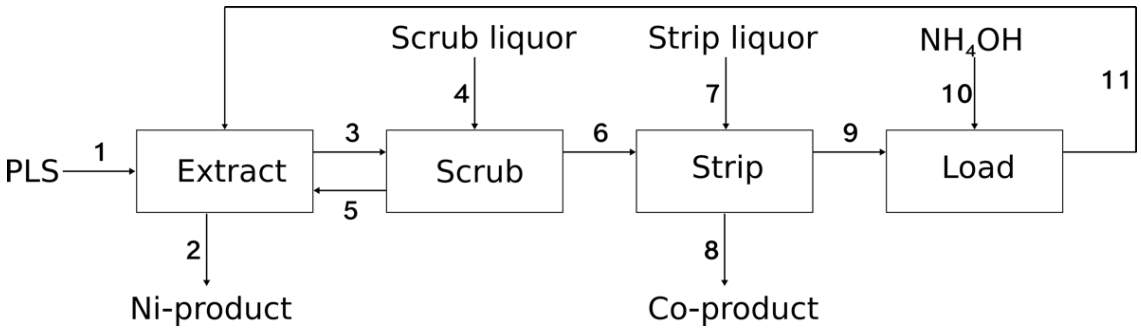

Figure 5-1. Pertraction refinery flowsheet to process cobalt for a PLS originating from spent hydro-treatment catalysts.

It was found that the most important mass resistance during PX stripping is located at the module and not due to reaction kinetics. Mass-transfer optimisation during stripping therefore requires further investigation using a hydrophilic membrane contactor.

Using a 0.1 M H_2SO_4 strip liquor, the Co product (8) contained of 5.52 g/L Co, whereas a 0.2 M solution resulted in a Co product containing 6.0 g/L Co. For this Co product, in order to obtain the required ≥ 50 g/L Co in the advance electrolyte, precipitation using NaOH can be used. During precipitation, using NaOH, Co precipitates as cobalt hydroxide. The precipitated Co salt can then be

redissolved, using the spent electrolyte (0.1 or 0.2 M H_2SO_4), to reach the target specification of 50 g/L. Alternatively, a 1 M H_2SO_4 solution can be used to obtain the target specification, as shown in Figure B-1. This solution, however, cannot be used as the advance Co electrolyte, due to the low acidity requirement for EW as discussed in Section 2.6. Intermediate Co products, on the other hand, such as carbonate or hydroxide salt can be produced from this solution. The preferred route subsequently depends on the desired product.

Lastly, the mass balance calculations for PX (which were used to calculate the metal concentration in the organic phases) required the removal of samples during PX experiments. During this study, the total sampling volume was kept under 5 % of the total sample volume to reduce the effect of sampling. To attain a more precise description of the mass transfer kinetics, a continuous concentration analysis method of the organic phases can be considered.

5.2.3) Conceptual design

During the course of this project a methodology was developed for the conceptual design of the extraction section of a PX Co-Ni refinery. From the results it was evident that, when using a 22 wt% C272 solvent, six Liqui-Cel™ 14x40 XF modules are required to reach the target Ni purity of ≥ 99.9 %. One such a module has a length of 1466 mm, a diameter of 356 mm and delivers a contact area of 373 m^2. Six of these modules, in series, subsequently delivers a contact area of 2238 m^2 in a volumetric space of 1.115 m^3. As stated previously, the model probably resulted in an overdesign of the column length which will ultimately lead to an increase in Ni co-extraction. A more advanced model, which considers pH changes occurring during the process, can be considered to reduce the Ni scrubbing effort. To further intensify the extraction PX section the following variables could be investigated:

- Temperature
- Aqueous and organic flow rates
- Type of membrane (hydrophilic vs. hydrophobic)
- Organic phase viscosity

After process optimisation, the same methodology applied in this project can be used for the straightforward conceptual design of the upgraded process. Additionally, the methodology can be used for the conceptual design of both the scrubbing and stripping sections after measuring the respective distribution isotherms.

APPENDIX A

Mass balance calculated for the Minemet PTY(LTD) PX plant.

Table A-1. Mass balance calculated for the Minemet PX plant. O/A ratio given in Table 4-1 was used (input parameters in bold).

Stream	PLS (1)	Ni Product (2)	Extract (3)	Scrub Liquor (4)	Scrub (5)	Scrubbed Extract (6)	Strip Liquor (7)	Co Product (8)	Stripped Solvent (9)	NH_4OH (10)	Loaded Solvent (11)
L/h	**200**	212.98	129.84	12.98	12.98	129.84	16.94	16.94	129.84		129.84
Co (g/L)	**4.235**	0.010	6.637	0	1.305	6.507	0	**50.00**	0	0	0
Ni (g/L)	**10.739**	9.882	0.543	0	2.118	0.013	0	0.100	0	0	0
C272 (g /L)	0	0	175	0	0	0	0	0	175	0	175
Co (kg/h)	0.847	0.002	0.862	0	0.017	0.845	0	0.845	0	0	0
Ni (kg/h)	2.148	2.105	0.070	0	0.028	0.002	0	0.002	0	0	0
NH_3 (kg /h)	0	1.230	0	0	0	0	0	0	0	1.230	1.230
C272 (kg /h)	0	0	22.74	0	0	22.74	0	0	22.74	0	22.74
Co-purity (%)	28.28	0.10	92.44		38.11	99.80		**99.80**			
Ni-purity (%)	71.72	**99.90**	7.56		61.89	0.20		0.20			
Notes	NH_4OH stream is lye: A 50% aqueous solution; NH_4^+ in Ni-product stream leaves as equivalent amount of $(NH_4)_2SO_4$. $(O/AQ)_{scrub}$ is assumed to be 10; co-extraction of Ni and co-scrubbing of Co are assumed to be 2% of the feed; stripping is assumed to be 100%										

APPENDIX B

Solution upgrading

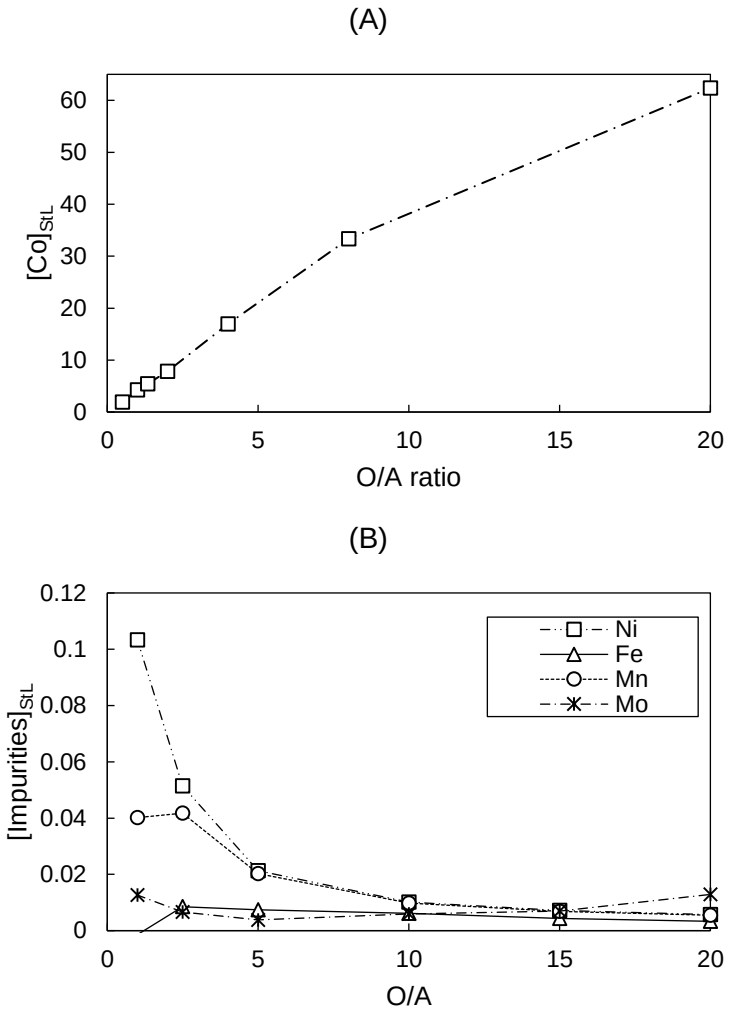

Figure B-1. Cobalt (A) and impurities (B) concentration in a 1M H_2SO_4 strip liquor as a function of O/A ratio.